ADVANCES IN INORGANIC CHEMISTRY, VOL. 38

DYNAMIC ELECTROCHEMISTRY OF IRON–SULFUR PROTEINS

FRASER A. ARMSTRONG

Department of Chemistry, University of California, Irvine, Irvine, California 92717

I. Introduction

Modern dynamic electrochemical methods[1] offer a powerful yet relatively inexpensive means for studying a variety of redox-active chemical systems. It is widely recognized that in addition to providing detailed thermodynamic and kinetic information, their use can yield valuable qualitative insight into aspects of complicated reactivities. Yet, while dynamic electrochemical techniques have made important contributions to coordination chemistry, even such now-standard meth-

[1] My use of the term "dynamic electrochemistry" refers to experiments in which one monitors a reaction via measurement of current (in this case a net flow of electrons) at the working electrode. There is a clear and important distinction to be made with "static electrochemistry," notably potentiometry, which is concerned with measurement of the position of equilibrium (i.e., the potential of zero net current) at the electrode.

ods as cyclic voltammetry have remained largely unexploited for the investigation of metal centers in proteins. Why? As I now hope to convey in this article, electrochemical methods afford interesting possibilities for exploring and quantitatively examining reactions of Fe–S clusters in both the time domain and the potential domain.

A major view that may account for the underuse of dynamic electrochemical methods for studying proteins reflects the experimental difficulties that are encountered. It is important to obtain a *direct* electrochemical response—that is, without the need for a mediator (typically a small, stable molecule displaying clean and reversible electrochemistry) to relay electrons between the protein's active site and the electrode. Generally speaking, the achievement of direct (i.e., unmediated) electrochemistry of various proteins has not proved straightforward. Two problems in particular have to be overcome (*1–3*). First, since redox centers in proteins tend to be shielded from the solvent by a variable intervening medium, electron exchange with an external redox agent depends upon the formation of a precursor assembly within which the two molecules are positioned so as to optimize electronic coupling (interaction between donor and acceptor wavefunctions). This requirement is serviced through noncovalent interactions involving a number of surface groups, and provides kinetic specificity in biological electron transfer (*4–6*). Clearly, in order to engage such selective macromolecules productively at an electrode, similar kinds of interactions need to be generated. Second, any such intimate association between electrode surface and protein must not cause denaturation, particularly if the denatured product remains adsorbed. This may occur, particularly if the protein is conformationally labile (*7*).

An alternative view is that the underuse of dynamic electrochemical methods for characterizing redox proteins reflects what is in my view an unfortunate misconception, namely, that such techniques provide the same information as may be obtained by mediated redox potentiometry. Naturally, so long as this notion persists, there exists little stimulus for the efforts necessary to achieve and interpret a direct, dynamic electrochemical response from a protein system. Indeed, for determining reduction potentials of uncomplicated redox couples, potentiometric methods are certainly more widely applicable (*8*).

In this article, I wish to provide some perception of the contribution that can be made by dynamic electrochemical methods toward the often difficult task of defining reactions of Fe–S clusters in a protein molecule. Despite the relatively modest amount of material published to date, these reports do show that such an approach, when combined with appropriate spectroscopic techniques, can yield valuable insight

that is not obtained readily or in acceptable detail by other means. Most of the work described has taken place in my own laboratory and in collaboration with other scientists. My emphasis is upon the detection and study of unusual or subtle features of reactivity, and I have not dwelled heavily upon studies that have focused upon voltammetry as an alternative to potentiometry. Although electrochemistry is both a broad and mathematically sophisticated field, it is covered in several excellent textbooks that provide clear descriptions of theory and experimental procedures (*9–12*). Thus only supplementary concepts and necessary clarification will be presented throughout the text.

II. Background

A. Some Recent Developments with Fe–S Clusters

Several significant developments have occurred during the past decade. Stemming from endeavors in various disciplines—molecular biology, spectroscopy, crystallography, and synthetic "model" chemistry—they are described in detail by other authors in this volume and only a brief summary is presented here.

1. A wide-reaching biological aspect is the realization that Fe–S clusters have important functions outside the established realm of electron transport (*13*). More specific catalytic roles are being established—most significantly in the area of nonredox enzymes. Due to the efforts of Beinert and his co-workers, much is now known about the structure and mechanism of aconitase, a dehydratase of the citric acid cycle, in which the active site [4Fe–4S] cluster catalyzes the interconversion between citrate and isocitrate (*14*). Most recently, evidence has been presented that suggests that Fe–S clusters may be involved directly in the genetic regulation of Fe levels in eukaryotic cells (*15, 16*).

2. The formulation of a class of clusters as [3Fe–4S] (essentially a [4Fe–4S] cubane with one Fe missing) is now established, following a decade of disagreement between the conclusions stemming from spectroscopy and crystallography (*17–24*).

3. There has been growing awareness of diversity in the modes of coordination of Fe–S clusters. In addition to cysteine thiolate, it is now clear that other protein donor groups can be ligands to Fe. For example, the "Rieske"-type [2Fe–2S] cluster is coordinated by two cysteine thiolate S atoms to one Fe and by two imidazole N atoms (histidine) to

the other (*25*). Exogenous (nonprotein) ligands may be coordinated. Aconitase provides such an example; here, one Fe of the [4Fe–4S] cluster is not bound to a protein donor but to OH^- (*26,27*). This "subsite-differentiated" Fe atom is also the site of substrate binding.

4. The ability of Fe–S clusters to alter their structure within certain protein hosts is now recognized. Specifically, several examples are established in which [3Fe–4S] and [4Fe–4S] clusters interconvert readily (*13, 14, 28–30*). In the case of aconitase, isolation under aerobic conditions induces release of the labile, subsite-differentiated Fe atom and loss of catalytic activity (*14*). Activation of the inactive enzyme involves addition of Fe(II) to the reduced $[3Fe–4S]^0$ cluster. Taking this theme further, it has recently been reported that the amino acid sequence of human iron-responsive element binding protein (IRE-BP), which regulates the expression of ferritin and of transferrin receptor, bears marked homology with sequence of aconitase (pig heart mitochondria) (*15, 16*). This has raised some speculation that interconversion between [3Fe–4S] and [4Fe–4S] clusters may provide a basis for sensing the Fe activity in the cytoplasm or an organelle.

5. There is spectroscopic evidence for the existence of Fe–S clusters having more than four Fe atoms (*31*).

6. Addition of metals other than Fe to [3Fe–4S] clusters has been demonstrated *in vitro* for certain proteins (*32–36*). Studies with such heterometal clusters are leading to a greater understanding of complex magnetic properties. There is also the possibility that heterometal clusters may be more widespread in nature than is currently recognized (we are already aware, for example, of the existence of Fe–Mo–S or Fe–V–S clusters as cofactors of nitrogenase) (*37, 38*).

7. Synthesis and characterization of "model" complexes has continued to be a powerful strategy for understanding the fundamental chemical and spectroscopic properties of Fe–S clusters. Efforts by Holm and others are now directed at achieving discrete, subtle variants of Fe–S clusters, creating what they have termed "subsite specific" systems, and examining their chemical and spectroscopic properties (*39–46*).

B. Problems Encountered in Studying Reactions of Fe–S Clusters in Proteins

These developments highlight the importance of *dynamic* properties that must be relevant to the *in vivo* functioning of clusters, particularly in catalysis or regulation. To gain a greater understanding of these aspects it is necessary to examine equilibria and kinetics of metal and ligand interchange, and to determine how these reactivities vary with

the cluster oxidation level (and, consequently, upon the electrochemical potential of the surrounding environment). Sensitive, quantitative measurements need to be made. Current strategies for studying reactions of Fe–S clusters in proteins are dominated by a general theme—that is, the preparation and spectroscopic examination of a sample in some stationary homogeneous state. Such a strategy focuses upon the characterization of structural, electronic, and magnetic properties of the isolated species. However, certain limitations are apparent. First, the most widely used spectroscopic methods for studying Fe–S clusters—electron paramagnetic resonance (EPR), electron–nuclear double resonance (ENDOR), Mössbauer, magnetic circular dichroism (MCD) and resonance Raman—each require the sample to be in the frozen state. To monitor reactions in the time domain at ambient temperature it is necessary to use nuclear magnetic resonance (NMR) or circular dichroism (CD), since absorption spectra of Fe–S species are typically broad and devoid of characteristic features. Second, in order to probe tight-binding equilibria (dissociation constants in the micromolar range or lower) it is necessary to make measurements with low concentrations of protein. However, most spectroscopic techniques require cluster concentrations that are higher than 50 μM. Third, sample preparation is often slow and is usually complicated by the need to manipulate sensitive materials under critical conditions of controlled potential.

C. Useful Features of Direct (Unmediated) Dynamic Electrochemistry

Dynamic electrochemical methods have several useful features for studies of redox proteins.

1. In appropriate cases, the voltammetric response (i.e., the voltage–current profile) constitutes a "signal" that can be assigned to a specific species (redox couple). For Fe–S clusters this is particularly useful since a convenient label is now provided. The usefulness continues for proteins that contain several clusters, provided their reduction potentials are sufficiently separated.

2. In the absence of a requirement for artificial redox mediators, electrochemistry is dynamically interactive and enables quantitative studies to be undertaken in the time domain. It is possible to transform and monitor states simultaneously under potential control, and to maneuver reversibly with respect to potential on short time scales. New species formed as a result of redox activity may be studied as coupled equilibria or "trapped," depending upon the electrochemical time scale.

3. The useful potential range is wide and continuous, being restricted only by the limits for electrical breakdown of the solvent or electrode surface and not by the properties of mediators or titrants. Voltammetry of neutral aqueous solutions at carbon electrodes is feasible at potentials more negative than -1 V and more positive than 0.8 V (all potentials given are versus the standard hydrogen electrode). By contrast, the useful lower limit for sodium dithionite, the most widely used biochemical reductant, is around -550 mV at pH 7 (*47*). As described later, voltammetry has been used to study chemically reversible redox transitions occurring at electrode potentials of -0.75 V or lower.

The above-mentioned features are generally applicable and have been exploited in several studies of Fe–S proteins. Even so, much more can be gained in terms of experimental refinement by restricting our observation to protein molecules that are immobilized at the electrode surface, i.e., not diffusing rapidly between the electrode and bulk solution. Since electron transfer is dependent upon specific protein–electrode interactions, an electrode surface that is not homogeneous may appear to an approaching protein molecule as an array of microelectrodes—that is, some areas being active (sites at which interaction leads to very fast electron transfer, i.e., reversible electrochemistry) and others being inactive (sites at which the protein does not interact in such a way, i.e., giving extremely irreversible electrochemistry) (*48–50*). In the limit of the entire electrode surface being active, the situation becomes that of linear diffusion to a planar macroelectrode and the voltammetric response conforms to the theory described by Nicholson and Shain (*51*). If, however, the fraction of active areas is small, the situation becomes that of radial diffusion to a microlectrode, and a steady-state voltammetric response (a sigmoidal wave) is obtained (*48*). The broad, poorly defined waveforms that are observed commonly for cyclic voltammetry of protein solutions may therefore be a combination of peaklike (linear diffusion) and sigmoidal (radial diffusion) waveforms.

Exploited with caution, the voltammetry of adsorbed protein molecules offers many important and useful features. The schematic shown in Fig. 1 illustrates what we can regard as an idealized situation. The concept is described as follows:

1. Redox-active protein molecules are adsorbed at an electrode surface. Electron transfer between the electrode and the protein's redox-active site(s) occurs reversibly.

2. Adsorption occurs with minimal conformational disruption and native functional properties are retained throughout the experimental

range of applied electrode potential. (While a large electric field can significantly alter the properties of a protein molecule, it should be borne in mind that fields of varying strength exist also at biological membranes.)

3. The coverage is monolayer or lower, and active sites in each protein molecule behave independently (but identically) to those in neighboring molecules.

Formation of such an array can depend critically upon conditions such as electrode surface preparation and modification, solution ionic composition and pH, and coadsorption of other complex molecules, as indicated by the triangular shapes in Fig. 1. Since the protein molecules are absent from the electrolyte solution and none effectively leaves the electrode surface, all the charge that passes across the protein–electrode interface is accounted for in what may be regarded as a closed system. Analysis of the observed voltammetric response yields quantitative information on reactivites of specific active sites—information that for very reactive systems may be difficult to obtain by more conventional methods.

Some specific advantages of studying protein molecules adsorbed as an electroactive monolayer/submonolayer are as follows:

1. The status of each redox-active site may be addressed on a rapid time scale. Unlike the situation in which the electrode contacts a "thick" solution of freely diffusing protein molecules, the voltammetric (linear sweep or cyclic) response that is observed for a well-behaved

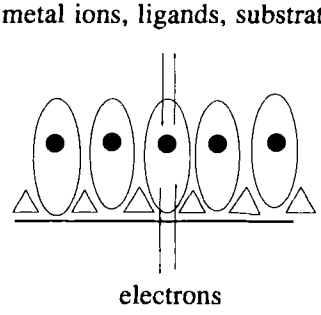

FIG. 1. Schematic illustrating a layer of protein and coadsorbate molecules strongly adsorbed at an electrode surface. In an ideal situation, redox-active sites behave independently of each other, exhibit reversible electrochemistry, and interact freely with reagents in the contacting electrolyte.

surface-confined system is compact and finite. Figure 2 illustrates the limiting (ideal) case described by Laviron, in which a reversible, diffusionless electron transfer reaction occurs uncomplicated by species heterogeneity, intersite interaction, or coupled chemistry (*52–54*). Peak potentials correspond to the formal reduction potential $E^{0'}$, the separation between reduction and oxidation peaks (ΔE_p) is 0 mV, and the theoretical peak width at half-height (δ) is $91/n$ mV at 25°C, where n is the number of electrons required to be transferred in the process.

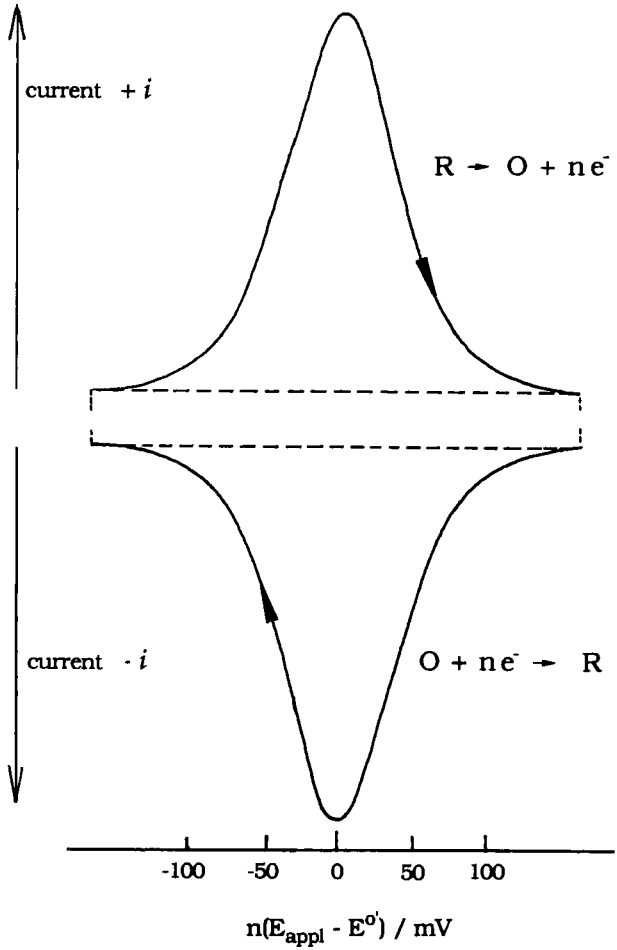

FIG. 2. Theoretical cyclic voltammogram for an ideal, reversible, electrode reaction of an adsorbed redox couple (see Refs. *52–54*).

2. For each redox couple, the following readily measured parameters are analytically useful: the area under the wave yields the total charge exchanged between the electrode and the active site (for multicentered proteins, ratios of areas of separate waves can yield the relative site stoichiometries); the parameter δ gives information on species heterogeneity and intersite interactions; and the standard rate constant (k^0) for electron exchange (if this falls short of being reversible) can be estimated from ΔE_p (*53, 54*). Complex waveforms arise if two or more redox couples have similar reduction potentials; however, these are more readily resolved than for the case of diffusing redox couples.

3. The amount of material required to form a monolayer at a typical electrode surface (0.2 cm^2) corresponds to a picomole or less. Thus a large number of experiments can be conducted with a limited supply of precious sample.

4. Sensitivity for determination of tight-binding equilibria is good. The small number of molecules under examination makes it possible to study and quantify reactions that occur between the protein active sites and reagents that are contained in the electrolyte at high dilution. In terms of this sensitivity to trace reagents, the philosophy bears resemblance to that of stripping voltammetry (*9–12*). Effects of solvents (such as glassing agents required for MCD spectroscopy) can also be screened, without risking sacrifice of a significant amount of precious material.

5. By analysis of the voltammetric response, it is possible to obtain kinetic information; this includes the rates of entry and release of reagents at specific centers.

6. If the adsorbed protein is an enzyme, the capability for precisely imposing a continuously variable electrode potential enables detailed examination of the potential dependence of catalytic function. Such an ability to fine tune the electrode potential (and thus vary the driving force for the electrode–protein electron transfer step) can lead to the detection of gating effects and the identification of redox-active groups that may regulate electron flow, depending upon their redox status.

Which techniques are most useful? Electrochemistry offers a wide selection. To date, direct current (DC) cyclic voltammetry has been the most widely used method, but as mentioned earlier, the linear sweep response obtained with a protein solution often consists of just a weak sigmoidal-like wave. Where greater current sensitivity and potential resolution are required, potential-step techniques, particularly square-wave voltammetry, offer considerable advantages since the response is greatly amplified by digital modulation of the potential sweep (*55*).

Recent examples of the application of square-wave voltammetry can be found in studies reported by Smith and co-workers, who have investigated reduction potentials for the $[4Fe–4S]^{2+/1+}$ couple in several bacterial ferredoxins (*56, 57*). For more refined kinetic measurements, techniques such as chronocoulometry, chronoabsorptometry, and rotating disk voltammetry are widely used by electrochemists and have been applied to protein electrochemistry (*58, 59*).

How reliable are direct, dynamic electrochemical techniques for determining reduction potentials? For a diffusion-controlled electrode reaction, agreement should be good provided reagents (promoters) that may be required to enable the protein to interact with the electrode do not bind to the protein in a way that either causes a conformational change or favors one redox state over another. Discrepancy is expected to be more significant for studies on adsorbed proteins. Feinberg and co-workers have compiled reduction potential data for *Clostridium pasteurianum* 2[4Fe–4S] ferredoxin as reported by a number of groups using different methods, including voltammetry, at various electrodes (*56, 57*). A spread of ~50 mV is observed, but this does not indicate any trend that distinguishes between equilibrium and dynamic electrochemistry.

D. Achieving Direct Electrochemistry of Ferredoxins

Several early reports described polarography of ferredoxins and observations of waves in the regions of applied electrode potential expected on the basis of equilibrium potentiometric measurements (*60–66*). The question of whether these waves reflected properties of adsorbed or diffusing molecules was debated. In their studies on the effects of solvent on the redox properties of *C. pasteurianum* 2[4Fe–4S] ferredoxin, Holm and co-workers concluded that the polarographic response was reversible; plots of $\log i/(i_d - i)$ against the applied potential E_{appl} gave gradients of -59 mV and half-widths of pulse polarographic waves were 90 mV, each as expected for a one-electron process (in this case two noninteracting redox sites) (*63*). The reduction (half-wave) potential thus obtained was -430 mV at pH 8.4, at the negative end of the range of values determined by potentiometry. Polarography is a technique in which the electrochemical response is recorded at short contact time; consequently extended time processes and the stability of the response are not addressed (*9–12*). The effect of extended contact with a mercury electrode was investigated by Ikeda and co-workers, who carried out cyclic voltammetry experiments on *Clostridium* ferredoxin at a hanging mercury drop electrode (*65*). The results showed

that the ferredoxin is adsorbed strongly and that the Fe–S clusters are rapidly degraded, giving rise to signals attributable to cysteine thiolate redox activity. This is not unexpected, given the well-known affinity of Hg for sulfur ligands (*67*).

In 1977, Hawkridge and co-workers discovered that quasi-reversible electrochemistry of a solution of spinach [2Fe–2S] ferredoxin could be achieved with a gold electrode that had been coated with an electrochemically polymerized form of methyl viologen (*58, 68*). Ferredoxins generally have p*I* values below 4 and carry significant negative charges at neutral pH. One likely rationale is therefore that the layer functions by providing a noninsulating positively charged surface that is suited for interaction with the protein surface. Bianco and co-workers and, more recently, Smith and Feinberg have employed this type of modified electrode to study ferredoxins; however, a small concentration of methyl viologen (10% of the protein) was required in solution (*56, 69*). Van Dijk and co-workers have also described results with a glassy carbon electrode modified by polymeric viologen (*70*).

In 1982, Hill and co-workers reported that quasi-reversible electrochemistry of *C. pasteurianum* 2[4Fe–4S] ferredoxin (Fd) could be obtained at pyrolytic graphite electrodes in the presence of Mg^{2+} ions (*71*). In a subsequent paper it was shown that the electrochemical response depended upon the electrode surface oxide density (polished edge > polished basal ≫ cleaved basal) and was promoted by metal aquo ions and a variety of complex cations, none of which are redox active in the potential range of the experiment (*72*). Many other proteins, including spinach [2Fe–2S] ferredoxin, were found to be similarly active, giving cyclic voltammetry that could be described as diffusion controlled. It was proposed that the cationic promoters function by forming salt-bridge-like cross-linkages between residues on the protein surface and the weakly acidic C–O groups of the electrode surface. By such interactions, the protein molecule can be held and oriented at the electrode in the manner of a precursor electron transfer complex. Such reagents may be thought of as greatly increasing the number of protein interaction sites on the electrode surface. Without promoters, the electrochemistry may still be reversible, but occur at few sites, thus resulting in a weak sigmoidal-like response as viewed by linear-sweep methods (*49*). Using square-wave voltammetry, Feinberg and coworkers have obtained an electrochemical response for a solution of *C. pasteurianum* Fd at a pyrolytic graphite edge (PGE) electrode without the addition of any ionic species apart from Tris/HCl and NaCl (*57*).

In 1988, it was reported that aminocyclitols such as neomycin or

tobramycin were much more effective than metal ions and complexes for promoting electrochemistry of ferredoxins (*73*). This was evident from a study of the cyclic voltammetry of *Azotobacter chroococcum* 7Fe ferredoxin at edge-oriented graphite (PGE). Aminocyclitols (also known as aminoglycosides) are a class of molecules that have useful antibiotic properties (*74*). A key feature undermining their effectiveness is that they contain a number of basic ($-NH_3^+$, $-NH_2R^+$) groups positioned at locations on a complex oligosaccharide. This spatial complexity probably suits them particularly well for interaction with residues on the protein surface and with irregular C–O sites on the electrode. They have since proved to be very effective with other ferredoxins (*29, 75, 76*). In addition to being redox inactive, they are also colorless and diamagnetic and thus do not interfere with spectroscopic examination of electrochemically transformed samples. A further development has been the discovery that they induce the formation of an electroactive film of protein molecules, effectively monolayer/submonolayer thickness, that can be transferred upon the electrode between various electrolyte solutions (*35, 36, 77*).

III. Applications

A. Redox Properties of *Azotobacter* Ferredoxin I and Site-Directed Mutant Forms

Studies with this protein serve to demonstrate the most obvious application of direct electrochemical methods, that is, the investigation of basic redox properties. Voltammetry provides advantages of rapidity, sample economy, and the ability to measure reduction potentials of redox couples that involve unstable species, either by virtue of intrinsic lability or oxygen sensitivity. Direct electrochemical methods are valuable for determining reduction potentials that are too negative to be addressed effectively by chemical titrants and mediators, and for preparing samples of highly reducing products for spectroscopic examination. They are also suited for extensive investigations, for example, in the measurement of $E^{0'}$ under a range of conditions of temperature or pH.

We have been interested in the redox properties of 7Fe ferredoxins from the N_2-fixing aerobe *Azotobacter*. The so-called ferredoxins I (Fd I) isolated from *Azotobacter vinelandii* or *A. chroococcum* each contain one [3Fe–4S] and one [4Fe–4S] cluster (*24*). The protein from *A. vinelandii* (polypeptide $M_r \sim 12{,}700$) has been particularly well

studied. The crystal structure of the oxidized form shows that the two clusters are ligated by seven out of a total of nine cysteine residues, according to the scheme shown in Fig. 3A (*21, 22*). At the present time, the amino acid sequence of *A. chroococcum* ferredoxin is not known.

Spectroscopic studies with Fd I isolated from *A. vinelandii* and *A. chroococcum* have shown that the two proteins possess very similar, unusual properties. In either case, the $[3Fe–4S]^0$ cluster generated upon one-electron reduction exists in two pH-interconvertible forms, each having a spin state $S = 2$, but exhibiting different low-temperature MCD spectra (*24, 78, 79*). The alkaline form (pH > 7) shows a spectrum that is very similar to that exhibited by $[3Fe–4S]^0$ clusters

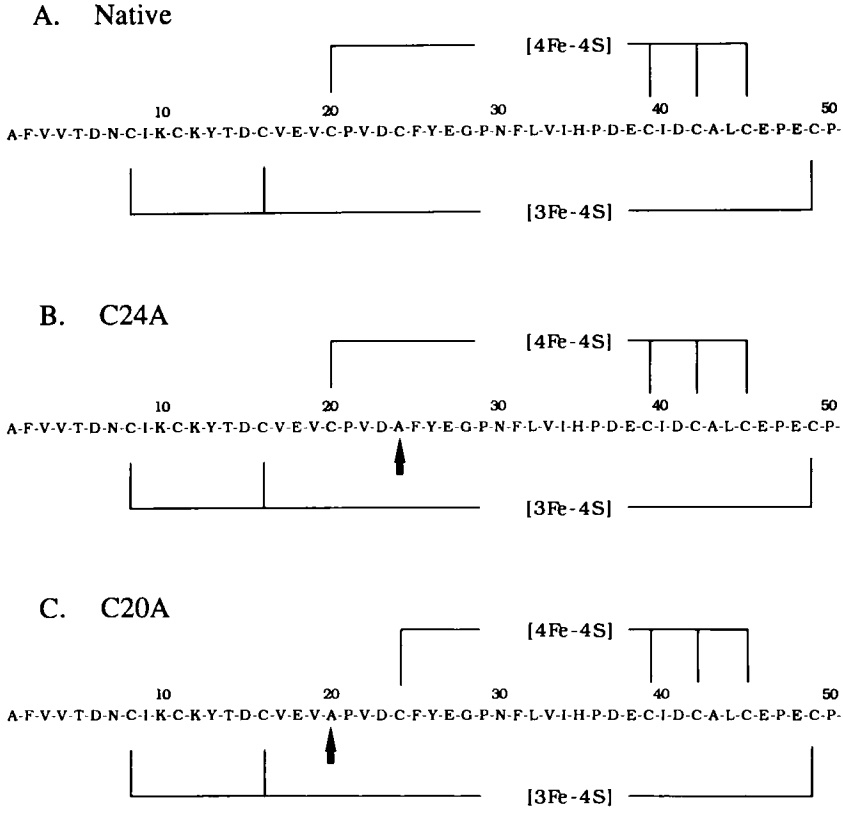

FIG. 3. Amino acid sequences of native *A. vinelandii* Fd I and the site-directed mutants C24A and C20A. Only amino acids 1–50 are shown since the second half of the polypeptide chain does not coordinate the clusters. Altered residues are indicated by arrows.

in other proteins, including inactive beef heart aconitase and the (so-called) ferredoxin II from *Desulfovibrio gigas* (*80, 81*). By contrast, the acid form shows an MCD spectrum which is unlike that observed for other proteins. By use of CD spectroscopy it has been shown (for *A. vinelandii* Fd I) that this difference persists at ambient temperature and in the absence of glassing agents (*24*).

It was known also that the [4Fe–4S] cluster in *A. vinelandii* or *A. chroococcum* Fd I is unusual in being nonreducible by dithionite at neutral pH. An earlier proposal that this was a high-potential iron–sulfur protein (HiPIP)-type cluster, i.e., operating between +3 and +2 oxidation levels, was shown to be in error (*82*). It was suggested instead that this was an unusual $[4Fe–4S]^{2+/1+}$ system for which $E^{0'}$ is more negative than −600 mV.

Direct electrochemical studies have provided a more detailed quantitative description of these anomalies. In the first such study, solutions of *A. chroococcum* Fd I at various pH values were examined by cyclic voltammetry at a PGE electrode (*73*). To promote the electrochemical response, millimolar levels of the aminocyclitols neomycin or tobramycin were included in the buffer electrolyte. Three redox couples, labeled A, B, and C, were observed, as shown in Fig. 4. At pH 8.3, the dominant wave pairs A and B appear of similar size. Couple A was shown to be quasi-reversible and to behave in the manner expected for an electrochemical process in which the current is limited by diffusion of molecules to a planar electrode surface; for example, a plot of peak current against $(\text{scan rate})^{1/2}$ was linear up to a scan rate of 100 mV/sec. Couple B was also observed to be electrochemically well-behaved. At pH values >7, where there is no interference from couple C, the electrode reaction appeared diffusion controlled up to at least 1 V/sec, while the peak separation remained <80 mV.

Assignments of couples A and B were made following spectroscopic examination of samples prepared by bulk electrolysis under controlled potential conditions. Small volumes (0.3–0.4 ml) of ferredoxin solutions can be electrochemically transformed conveniently using cells in which (in order to obtain a large surface area) the PGE electrode forms both the base and walls. Exhaustive reduction at an applied potential of −550 mV consumed one electron per molecule of protein and produced a product showing complete bleaching of the $g = 2.01$ EPR spectrum due to $[3Fe–4S]^{1+}$. A similar product, giving rise to the pH-dependent MCD spectra assigned as $[3Fe–4S]^{0}$, could be prepared by reduction with sodium dithionite. In this way, couple A was established to be due to the $[3Fe–4S]^{1+/0}$ cluster. Observed reduction potentials $E^{0'}_{obs}$ (deter-

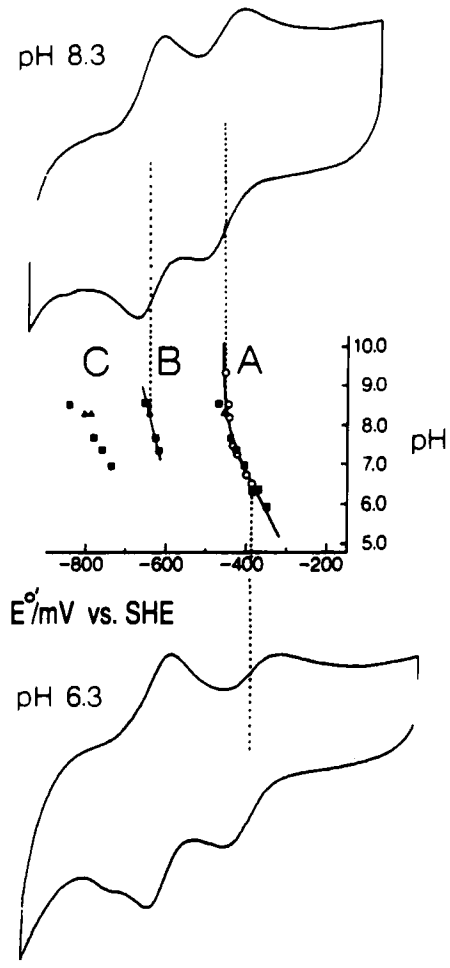

FIG. 4. Cyclic voltammetry of *A. chroococcum* Fd I at pH 8.3 {84 μM protein in 20 mM 3-[tris(hydroxymethyl)methylamino]-1-propanesulfonic acid, 0.1 M NaCl, 1.5 mM neomycin} and pH 6.3 [85 μM protein in 20 mM 1,4-piperazinebis(ethanesulfonic acid), 0.1 M NaCl, 1 mM tobramycin]. Temperature 3°C, scan rate 10 mV/sec. Electrode is PGE. Shown at the center is the pH dependence of $E^{0'}$ values. [Adapted from Armstrong, F. A., George, S. J., Thomson, A. J., and Yates, M. G., *FEBS Lett.* **234**, 107 (1988), with permission].

mined from the average peak potentials for reduction and oxidation waves) were pH dependent and data gave a good fit to Eq. (1),

$$E^{0'}_{obs} = E^{0'}_{alk} + (2.3RT/F)\log\{1 + [H^+]/K_H\} \quad (1)$$

which describes a system comprising the reactions given by Eqs. (2) and (3)) in which electron transfer is coupled to net addition of one H^+ to the reduced form, equilibrium being established rapidly and within the voltammetric scan time.

$$[3Fe\text{–}4S]^{1+} + e^- \rightleftharpoons [3Fe\text{–}4S]^0 \qquad E^{0'}_{alk} \quad (2)$$

$$[3Fe\text{–}4S]^0 + H^+ \rightleftharpoons [3Fe\text{–}4S]^0\text{---}H^+ \qquad 1/K_H \quad (3)$$

Under the conditions of the voltammetric measurements (temperature 3°C, 0.1 *M* NaCl as supporting electrolyte, 5 m*M* mixed-buffer system) the p*K* ($-\log K_H$) was determined to be 7.8 ± 0.1, with $E^{0'}_{alk} = -460$ mV and $\Delta E^{0'}_{obs}/d(pH) = -55$ mV (i.e., consistent with net addition of one bound H^+ per protein molecule. Such direct coupling to a proton transfer process is unusual for Fe–S clusters.

Anaerobic controlled potential electrolysis at −835 mV of a pH 8.3 solution consumed two electrons per protein molecule. Cyclic voltammetry of this product confirmed full retention of couples A and B, thus showing that no significant irreversible changes had occurred to the sample upon electrolysis. The EPR spectrum was complicated, being of the "$g = 1.94$" type with additional features and arising from 0.8 spin per molecule. It was similar to that of the two-electron reduced 7Fe ferredoxin from *Thermus thermophilus*, which contains a $[4Fe\text{–}4S]^{1+}$ cluster that is spin coupled to $[3Fe\text{–}4S]^0$ (*83*). Couple B could thus be assigned to the $[4Fe\text{–}4S]^{2+/1+}$ cluster. The mild pH dependence [$dE^{0'}/d(pH) = -25$ mV] suggested weak coupling to a protonation equilibrium. At pH 8.3, $E^{0'}$ was determined to be −645 mV, thus explaining why the reduced form could not be obtained by reduction with dithionite and confirming the earlier suggestion by Morgan *et al.* (*82*). It is worth noting that the bulk electrolysis approaches being quantitative even at the very low potentials used, and that the reduced $[4Fe\text{–}4S]^{1+}$ cluster does not react with water at any significant rate.

Couple C, a relatively minor feature in this case, has appeared to be a typical feature of ferredoxins that contain a [3Fe–4S] cluster. For most proteins (see below) we have found it to be a chemically complex process that occurs readily only for protein molecules that are confined to the electrode surface. As outlined later, some clarification of the nature of this redox couple has arisen from voltammetry of protein films in the absence of freely diffusing molecules.

A long-standing question, highlighted by the results obtained with *A. chroococcum* Fd I, is the origin of the large variation in reduction potentials of [4Fe–4S] clusters among different proteins (*84*). Most vividly of course, there exist two distinct classes of protein that display redox couples involving different pairs of oxidation levels. For the $[4Fe–4S]^{2+/1+}$ couple (as exhibited by ferredoxins), $E^{0'}$ values cover the range -250 to -650 mV, whereas for HiPIPs ($[4Fe–4S]^{3+/2+}$), $E^{0'}$ values range between $+50$ and $+450$ mV. It is found that ferredoxins do not exhibit the $+3$ oxidation level. A search for oxidation processes occurring at *C. pasteurianum* 2[4Fe–4S] ferredoxin using differential pulse and square-wave voltammetry revealed only reactions generating rapidly decomposing species (*85*). The first of these reactions, suggested to be the couple $[4Fe–4S]^{3+/2+}$ (product lifetime <2 msec) is associated with a reduction potential estimated at 850 mV. Conversely, there is no evidence to show that HiPIPs can attain the $+1$ oxidation level under physiologically feasible conditions. In what has been a much-cited experiment, Cammack showed that the $[4Fe–4S]^{2+}$ cluster in *Chromatium vinosum* HiPIP becomes reducible by dithionite (i.e., "ferredoxin-like") if the protein is unfolded in 80% dimethyl sulfoxide (DMSO) (*86*). Cyclic voltammetry of *C. vinosum* HiPIP under normal conditions failed to find any evidence for the $[4Fe–4S]^{2+/2+}$ couple at electrode potentials as negative as -1.2 V (*87*).

On the basis of detailed comparisons of the resonance Raman and crystallographic structures of several ferredoxins and several HiPIPs, it has been concluded that the two classes of proteins are distinguished by major differences in the local environment of the [4Fe–4S] cluster (*84*). These differences are the number of N—H···S hydrogen bonds (five in HiPIP against eight in Fds—the greater number stabilizing the electron-rich $+1$ oxidation level), the cysteine torsional angles (larger in HiPIP), the positions of cysteine residues in the sequence, and the degree of solvent accessibility of the cluster (much less in HiPIP). However, it has also been concluded that *within* each class there is remarkably little difference in these parameters. The question of the extent to which reduction potentials are modulated electrostatically by the presence of charged residues is an obvious one. Consider the $+1$ oxidation level, which with tetrathiolate ligation has a local charge of -3; this should be destabilized by the close proximity of a negative charge but should be stabilized by a nearby positive charge. It was suggested that while the nature of the amino acids close to the cluster must be influential in modulating the reduction potential, the *charge* on these groups should be unimportant since charged residues tend to be located on the protein surface (*84*). It is well known that reduction

potentials are modulated by protonation, although marked effects are rare for Fe–S clusters. For *A. chroococcum*/*A. vinelandii* Fd I, the combined voltammetric/MCD evidence provides strong evidence that site of protonation is very near or indeed at the $[3Fe–4S]^0$ cluster (*24, 73, 78, 79*). Another demonstration of the influence of a proton is given in a report by Smith and Feinberg (*56*). From voltammetric studies on several 2[4Fe–4S] ferredoxins, it was noted that one example (*Clostridium thermosaccharolyticum* Fd) showed a sigmoidal relationship between $E^{0'}$ and pH. The perturbation, approximately 40 mV in total, was attributed to redox-linked protonation of an adjacent histidine residue that is absent from the sequence of other bacterial ferredoxins. Systemmatic studies of subsite-differentiated cluster analogs have shed light upon the influence of intrinsic factors. Valence localization [Fe(III) character versus Fe(II)-type character] and ligand type (electron donor strength, monodentate versus bidentate) have each been shown to modulate the reduction potential (*40–42*).

To gain a more systematic understanding of how the redox properties and stabilities of Fe–S centers are influenced by the protein structure, Burgess and co-workers have used site-directed mutagenesis to alter specific amino acid residues in ferredoxin I from *A. vinelandii* (*76*). Mutant forms of this Fd I were expressed and isolated, then crystals were examined by X-ray diffraction in order to compare their structures with that of the native protein. In the two examples to be described, cysteine residues close to the [4Fe–4S] cluster were replaced by Ala, as shown in Fig. 3 (B and C). In the case of the C24A mutant, a nonligating Cys that is in van der Waals contact with the [4Fe–4S] cluster is replaced by alanine, but the resulting environment in the vicinity of the cluster is otherwise very similar to that of the native form (*88*). For the C20A mutant a ligating Cys is replaced; the cluster instead adopts Cys 24 and there is a large rearrangement of the local structure (*89*).

Electrochemistry was performed with ~0.1 m*M* ferredoxin solutions over a range of conditions of pH, using tobramycin or neomycin to promote interaction of the protein with the PGE electrode. Square-wave voltammograms of native, C20A, and C24A forms at pH 7.8 are shown in Fig. 5. As evidenced by the excellent alignment of couples A and C, the [3Fe–4S] cluster appears unperturbed. By contrast, the position of couple B, assigned as $[4Fe–4S]^{2+/1+}$ by analogy with *A. chroococcum* Fd I, varies over a range of ~150 mV. Collective data are given in Table I.

Further refinement stemmed from measurements of the pH dependence of $E^{0'}$ values for each couple. As shown in Fig. 6, data for couple A ($[3Fe–4S]^{1+/0}$) overlay and yield essentially indistinguishable values

TABLE I

REDUCTION POTENTIALS $E^{0'}_{obs}$ FOR THE Fe–S CLUSTERS OF NATIVE, C20A, AND C24A FORMS OF *Azotobacter vinelandii* FERREDOXIN I AS DETERMINED BY SQUARE-WAVE VOLTAMMETRY[a]

Couple	Protein	$E^{0'}_{obs}$ (pH 7.8) (mV)	$-d(E)/d(pH)_{obs}$ (mV)	$-d(E)/d(pH)_{lim}$ (mV)	pK	$E^{0'}_{alk}$ (mV)
$[3Fe–4S]^{1+\ 0}$ (= A)	Native	−425 (±5)	—	43 (+4)	7.8 (+0.2)	−445 (+15)
	C20A	−429 (±5)	—	42 (+3)	7.6 (+0.2)	−440 (+15)
	C24A	−427 (±5)	—	43 (+4)	7.9 (+0.2)	−449 (+15)
$[4Fe–4S]^{2+\ 1+}$ (= B)	Native	−647 (±5)	16	—	—	—
	C20A	−746 (±10)	15	—	—	—
	C24A	−600 (±5)	18	—	—	—
C	Native	−772 (±15)	—	—	—	—
	C24A	−782 (±5)	52	—	—	—

[a] All measurements made at 3°C. Data taken from Ref. *76*.

of pK, $dE^{0'}_{obs}/d(pH)$, and $E^{0'}_{alk}$ as analyzed according to Eq. (1). The result is consistent with the conclusion, drawn from the crystallography studies, that the alterations caused in the [4Fe–4S] cluster binding domain induce no significant structural changes close to the [3Fe–4S] cluster (*88, 89*). The center-to-center distance between clusters is 11 Å.

Data for couple B yield a set of essentially parallel straight lines having slopes $dE^{0'}_{obs}/d(pH)$ of approximately −16 mV. The increase in $E^{0'}$ of ~50 mV upon replacement of Cys 24 by alanine, in comparing what are otherwise very similar cluster environments, suggests that the noncoordinating cysteine in native *A. vinelandii* Fd I might be ionized (i.e., exist as the thiolate anion) throughout this pH range. While this may be considered unlikely, removal of a unit negative charge from a distance of van der Waals contact would certainly be expected to stabilize the reduced form of the cluster. On the other hand, the ~100-mV *decrease* in $E^{0'}$ observed upon replacement of Cys 20 by alanine shows that the advantage of removing the neighboring cysteine is outweighed considerably by effects due to the structural changes thus induced. Several factors are clearly involved. What is interesting, however, is that the C20A mutation produces no change in the exposure of the [4Fe–4S] cluster to solvent molecules, and that the number, type, and distances of NH···S hydrogen bonds are unchanged (although there are significant changes elsewhere).

The physiological function of Fd I is not known. The finding by Burgess' group that double-mutant strains C20A/Fld$^-$ and C24A/Fld$^-$ (Fld$^-$ strains do not synthesize flavodoxin) grow at the same rate as wild-type cells is interesting, since it raises the question of the physio-

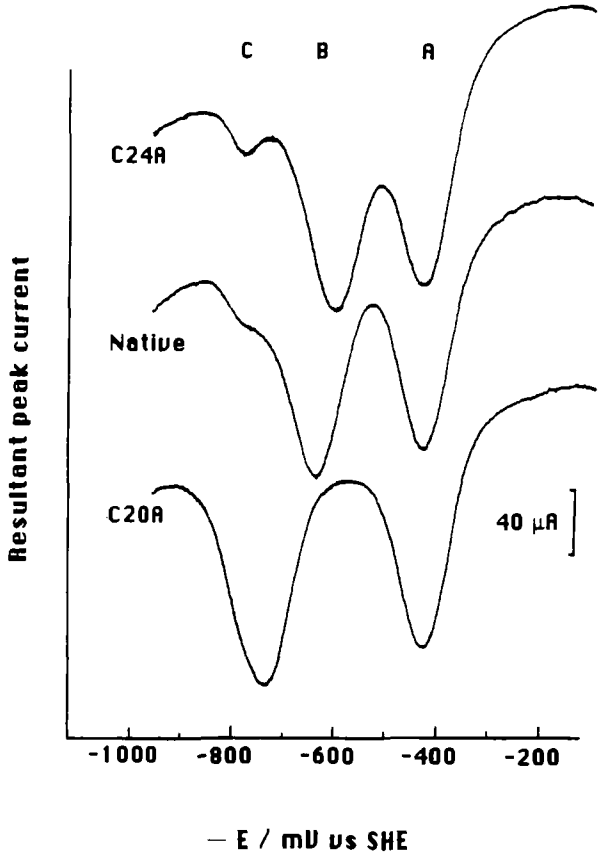

FIG. 5. Square-wave voltammetry of native *A. vinelandii* Fd I and site-directed mutants at a PGE electrode. Shown are resultant peak currents for scans made in the direction of increasing negative potential. Protein concentrations are 100 μM each in 0.1 *M* NaCl, 20 m*M* mixed buffer, pH 7.8. Temperature 3°C. Square-wave frequency is 60 Hz, pulse amplitude is 40 mV, potential step size is 1 mV. [Adapted from Iismaa, S. E., Vázquez, A. E., Jensen, G. M., Stephens, P. J., Butt, J. N., Armstrong, F. A., and Burgess, B. K., *J. Biol. Chem.* **266,** 21563 (1991), with permission.]

FIG. 6. Graph of $E^{0'}_{obs}$ against pH for redox couples A, B, and C of native *A. vinelandii* Fd I (○) and site-directed mutants C20A (△) and C24A (□). All data obtained at 3°C, 0.1 *M* NaCl, 20 m*M* mixed buffer, 1–2 m*M* neomycin or tobramycin. Graph A shows nonlinear regression fit to Eq. (1). Graphs B and C show best linear fits. [Adapted from Iismaa, S. E., Vázquez, A. E., Jensen, G. M., Stephens, P. J., Butt, J. N., Armstrong, F. A., and Burgess, B. K., *J. Biol. Chem.* **266,** 21563 (1991), with permission.]

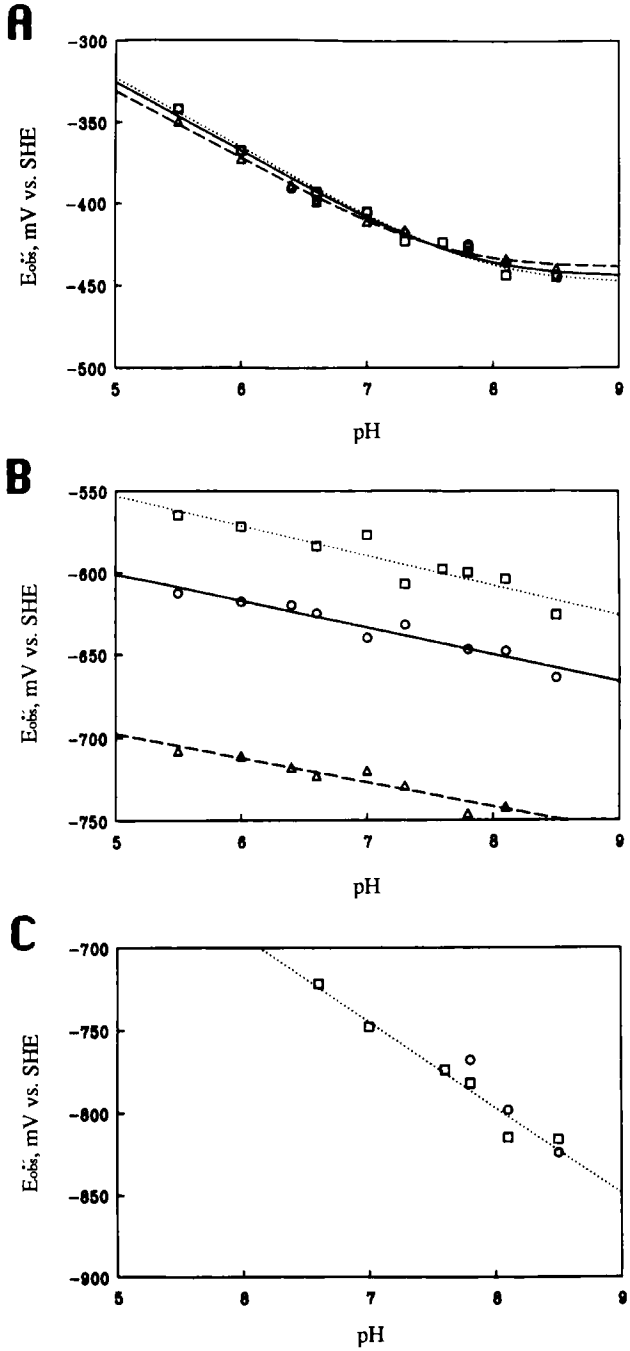
A
-300
-350
-400
-450
-500
5
6
7
8
9
Eobs, mV vs. SHE
pH
B
-550
-600
-650
-700
-750
5
6
7
8
9
Eobs, mV vs. SHE
pH
C
-700
-750
-800
-850
-900
5
6
7
8
9
Eobs, mV vs. SHE
pH

logical relevance of the very low-potential $[4Fe–4S]^{2+/1+}$ cluster (*76*). If it does indeed function as a redox center, its reduction *in vivo* requires that the natural electron donor has a reduction potential lower than −750 mV or that the process is coupled to an exergonic process such as ATP hydrolysis.

B. Characterizing the Fe–S Clusters in *Desulfovibrio africanus* Ferredoxin III, a Protein Containing a Reactive [3Fe–4S] Cluster

Ferredoxin III from *Desulfovibrio africanus* has proved to be an interesting subject for studying facile metal ion and ligand exchange reactions at clusters. As isolated, this small protein (polypeptide $M_r \sim 6600$) was found to contain seven or eight Fe atoms and seven or eight labile sulfides per molecule and to possess a total of seven cysteines occupying positions in the amino acid sequence as shown in Fig. 7 (*90*). In this schematic, the two clusters have been included in positions that we now believe to be correct, although support from crystal structure determination has yet to be obtained. Early attempts to characterize the clusters in *D. africanus* Fd III had met with limited success. From EPR spectroscopy it was known that the oxidized protein, as isolated, contains a $[3Fe–4S]^{1+}$ cluster, while spectra measured for a dithionite-reduced sample revealed the presence of $[4Fe–4S]^{1+}$. However, a satisfactory quantitative analysis was not obtained. Inspection of spectra obtained during conventional potentiometric titrations at various degrees of reduction revealed complex changes in spectral appearance and indicated that irreversible transformations were occurring.

As with *Azotobacter* ferredoxins, direct electrochemistry of a solution of *D. africanus* Fd III could be achieved readily with a PGE electrode

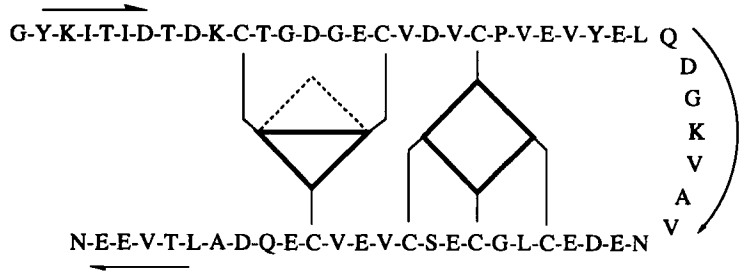

FIG. 7. Amino acid sequence of *D. africanus* Fd III showing proposed coordination of [3Fe–4S] and [4Fe–4S] clusters in the isolated 7Fe form.

in the presence of neomycin (*75*). Cyclic voltammetry under slow scan rate conditions (<20 mV/sec) showed two prominent pairs of waves (A and B) and a third weaker feature (C). This is displayed in Fig. 8. Couples A and B are of similar magnitude, provided (1) the scan rate is not increased (in which case waves A collapse to become a weak sigmoidal feature, eventually revealing an underlying adsorption wave at scan rates >160 mV/sec) and (2) provided a metal chelator such as EGTA is present in solution (in this case, EGTA is used instead of EDTA since the voltammetric response of FeEDTA interferes with

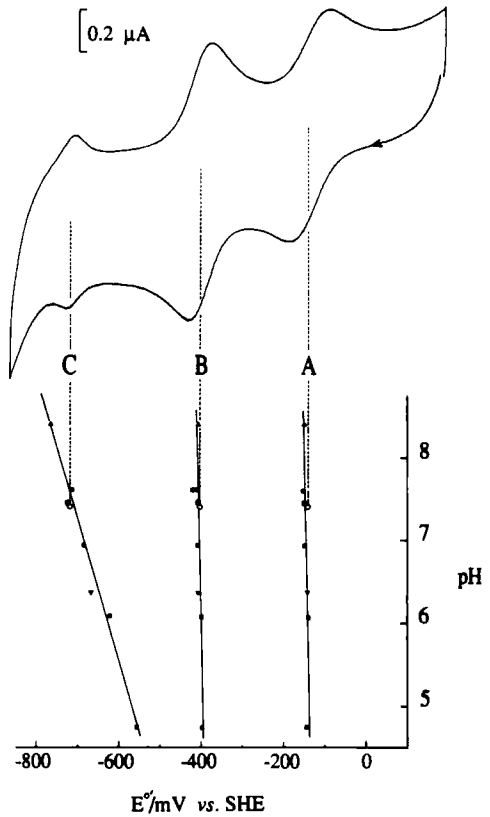

FIG. 8. Top: cyclic voltammetry of a solution of *D. africanus* Fd III at a PGE electrode showing couples A, B, and C. Protein concentration is 110 μM in 0.1 M $NaClO_4$, 20 mM HEPES buffer, 0.1 mM EGTA, 1.1 mM neomycin, at pH 7.4. Temperature 2°C, scan rate 8 mV/sec. Bottom: pH dependence of $E^{0'}$ values, various buffer electrolytes used. Lines are least-squares fits to data. [Adapted from Armstrong, F. A., George, S. J., Cammack, R., Hatchikian, E. C., and Thomson, A. J., *Biochem. J.* **264,** 265 (1989), with permission.]

couple A). The first observation is still unanswered [by contrast, couple B behaves much more classically in terms of exhibiting a linear relation between peak current and (scan rate)$^{1/2}$ up to 800 mV/sec, and ΔE_p values of 55–60 mV]. Further experiments (see below) have provided an explanation for the second observation in terms of a rapid reaction of the reduced ([3Fe–4S]^0) cluster with traces of Fe(II) liberated by slow, continual protein decomposition.

Couples A ($E^{0'} = -140$ mV) and B ($E^{0'} = -410$ mV) were each assigned by performing bulk electrolyses at controlled potential, and then examining the products by EPR and MCD. Exhaustive reduction at -260 mV in the presence of an equivalent of EGTA consumed one (0.9) electron per molecule. The resulting sample showed almost complete loss of the EPR signal at $g = 2.01$ and the appearance of a broad feature at $g = 12$. The MCD of the one-electron reduced protein is very similar to that of [3Fe–4S]^0 clusters in other proteins (*91*). Exhaustive reduction at a potential of -605 mV consumed two electrons per molecule and samples thus prepared showed (in addition to the $g = 12$ feature) an axial EPR spectrum with g values $g_\perp = 1.93$, $g_\parallel = 2.05$. Double integration of the high-field signal yielded values averaging 1.0 ± 0.1 spins. Couples A and B were thus assigned as [3Fe–4S]$^{1+/0}$ and [4Fe–4S]$^{2+/1+}$, respectively. Experiments carried out over the pH range 5–8 showed that neither couple exhibits a significant pH dependence (cf. the [3Fe–4S]$^{1+/0}$ cluster of *A. chroococcum*/*A. vinelandii* Fd I). Couple C appeared to be a kinetically complex pH-dependent redox couple, resembling the observation made for *A. chroococcum*/*A. vinelandii* Fd I.

From their respective spectroscopic similarities to [3Fe–4S] and [4Fe–4S] clusters in other proteins, positions in the protein were assigned as indicated in Fig. 7. The partial sequences -C-Xaa-Xaa-C-Xaa-Xaa-C- and remote -C-P- form a characteristic binding motif for [4Fe–4S] clusters in ferredoxins (*92*). The remaining three cysteine residues, located in the partial sequences -C-Xaa-Xaa-D-Xaa-Xaa-C and remote -C-E- were assigned to the [3Fe–4S] cluster. The resulting binding domain resembles that of a [4Fe–4S] domain except that an aspartate occupies the normal central cysteine position, and the remote cysteine that is normally followed by the kink former proline is followed instead by glutamate. Marked changes in the cyclic voltammetry are observed upon addition of two equivalents of Fe(II), i.e., sufficient to complex with the EGTA and react 1:1 with the ferredoxin (*29*). As shown in Fig. 9, reduction of the [3Fe–4S]$^{1+}$ cluster initiates its transformation into another species. Continued cycling results in complete disappearance of couples A and C and an apparent twofold increase in

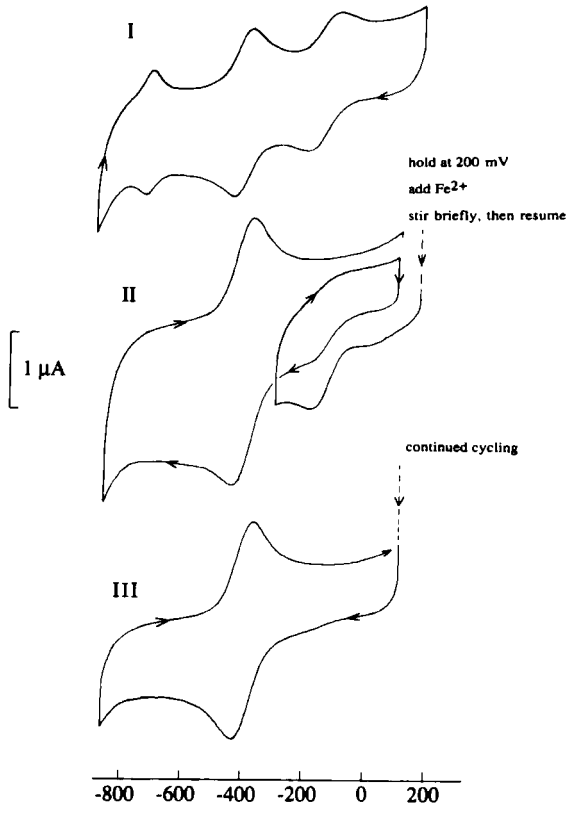

FIG. 9. Cyclic voltammetry of a solution of *D. africanus* Fd III showing the effect of adding Fe(II) to the electrolyte. Protein concentration was 110 μM in electrolyte composed of 0.1 M $NaClO_4$, 20 mM HEPES, 0.1 mM EGTA, 1.1 mM neomycin. At stage II, Fe(II) was added to give a total concentration of 0.21 mM. Scan rate 16 mV/sec. Temperature 2°C. [Adapted from George, S. J., Armstrong, F. A., Hatchikian, E. C., and Thomson, A. J., *Biochem. J.* **264,** 275 (1989), with permission.]

the amplitude of couple B. For the resulting product, peak currents were observed to be proportional to scan rate up to at least 160 mV/sec and the peak-to-peak separation was 60 mV at 16 mV/sec. The waveshape conforms closely to that expected for a single one-electron couple with $E^{0'} = -400$ mV, or more than one such couple having reduction potentials very close in value. Similar results were obtained in different electrolyte media, for example 0.1 M $NaClO_4$ instead of NaCl, and pH 6.3 [4-(2-hydroxyethyl)-1-piperazineethanesulfonic acid

(HEPES)] or pH 8.3 {3-[tris(hydroxymethyl)methylamino]-1-propanesulfonic acid (TAPS)}.

A quantitative analysis of this transformation was undertaken by performing bulk electrolysis prior to, during, and following addition of Fe(II) to the sample solution. The course of one such determination is shown in Fig. 10. A solution of *D. africanus* Fd III containing one equivalent of EGTA was exhaustively reduced at −610 mV. This consumed two electrons per molecule. Then aliquots of Fe(II) [each corresponding to approximately 0.25 Fe(II) per protein molecule] were injected into the stirred cell while the electrode potential was maintained at −610 mV. The first two additions produced little change because the Fe(II) is complexed preferentially by the remaining EGTA, but several subsequent additions resulted in large increases in current until a

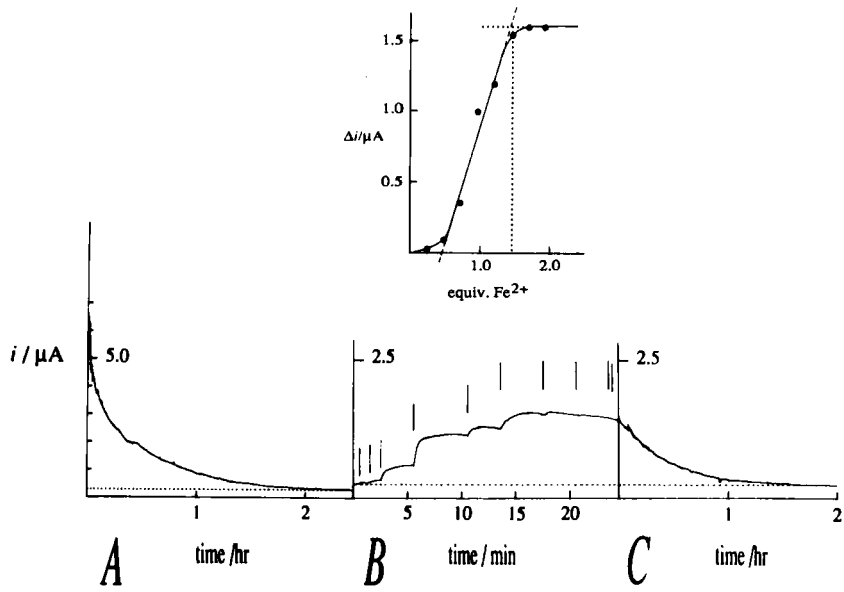

FIG. 10. Bulk electrolytic reduction of *D. africanus* Fd III and titration with Fe(II). (A) Bulk reduction at −610 mV in stirred cell. Solution is 0.4 ml containing 110 μM protein in 0.1 M NaCl, 20 mM HEPES, 0.1 mM EGTA, 1.5 mM neomycin, pH 7.4. Temperature 3°C. (B) Additions of 0.25 equivalents of Fe(II) to the two-electron-reduced protein while holding applied potential at −610 mV. Graph shows the increase in current observed as a function of the number of equivalents of Fe(II) added. The line drawn through the central points corresponds to a predicted uptake of 1.0 equivalent Fe(II) per protein molecule, following the initial lag due to complexation by EGTA. (C) Further bulk reduction at −610 mV, following from B. [Adapted from George, S. J., Armstrong, F. A., Hatchikian, E. C., and Thomson, A. J., *Biochem. J.* **264**, 275 (1989), with permission.]

limiting value was reached. Analysis of the Fe(II) titration showed that one Fe(II) was taken up per protein molecule. The solution was then electrolyzed further to equilibrium. Determination of the charge passed in this second phase was consistent with addition of one further electron per protein molecule.

The products of this reaction [and of chemically transformed samples prepared by addition of Fe(II) and variable amounts of dithionite to the 7Fe protein] were examined by EPR and MCD spectroscopy. The spectrum of the oxidized product [formed by reducing with one electron equivalent of dithionite, then adding Fe(II)] showed no significant EPR signals. In the UV-visible spectrum, the 408-nm shoulder exhibited by the 7Fe protein was replaced by a rounded peak at 390 nm, similar to that observed for ferredoxins containing only [4Fe–4S] clusters. MCD spectroscopy showed that this product was diamagnetic. The EPR spectra of the partial and fully reduced products were interesting. A rhombic signal with g values 2.05, 1.93, and 1.89 was observed upon reduction by <0.5 electron equivalents. Upon complete reduction (i.e., by two electron equivalents) the spectrum appeared more complicated, indicative of spin coupling to a nearby paramagnet. However, double integration of the low-field signals yielded only a single spin per molecule, leaving one spin unaccounted for. The other clearly distinguished feature in the spectrum was a signal at $g = 5.27$, and this was assigned to a major species with spin $S = \frac{3}{2}$. The MCD spectrum was very different from that of the $[3Fe–4S]^0$ cluster, but similar in feature to those of other $[4Fe–4S]^{1+}$ cluster-containing proteins. Its intensity was greater than expected for two $S = \frac{1}{2}$ $[4Fe–4S]^{1+}$ clusters, and the form of the resulting magnetization curve indicated the presence of species having $S > \frac{1}{2}$.

Together, the results from these experiments suggested a sequence of reactions [Eqs. (4)–(6)] in which Fe(II) enters the reduced $[3Fe–4S]^0$ cluster rapidly to complete a cubane-type $[4Fe–4S]^{2+}$ structure, which can undergo further one-electron reduction. No reaction occurs with the oxidized $[3Fe–4S]^{1+}$ cluster. Such a scheme resembles the *in vitro* activation of aconitase (*14*). The reactivity also explained the problems involved in characterizing the 7Fe protein, which is subject to slow degradation accompanied by loss of Fe.

$$[3Fe–4S]^{1+} + e^- \rightleftharpoons [3Fe–4S]^0 \qquad E^{0'} = -140\ \text{mV} \tag{4}$$

$$[3Fe–4S]^0 + \text{Fe(II)} \rightarrow [4Fe–4S]^{2+} \qquad \text{fast} \tag{5}$$

$$[4Fe–4S]^{2+} + e^- \rightleftharpoons [4Fe–4S]^{1+} \qquad E^{0'} = \sim -400\ \text{mV} \tag{6}$$

The resulting product is an 8Fe ferredoxin containing two [4Fe–4S] clusters. However, unlike *C. pasteurianum* Fd, one of the clusters must lack a cysteine thiolate donor. The question of the nature of the nonthiolate ligand is not yet answered, although a water molecule (H_2O/OH^-) and the carboxylate function of Asp 14 are the primary possibilities. Several other ferredoxins containing a [3Fe–4S] cluster are known to have a partial sequence –C–Xaa–Xaa–D–Xaa–Xaa–C– similar to that of *D. africanus* Fd III. The most notable of these is the unusual ferredoxin isolated from the hyperthermophile *Pyrococcus furiosus* (*30*). This protein is a monomer (polypeptide $M_r \sim 7500$), containing a single [4Fe–4S] cluster that is readily degraded to a [3Fe–4S] cluster if isolated under aerobic conditions. Like *D. africanus* Fd III, the reduced $[3Fe–4S]^0$ cluster takes up Fe(II), but in this case the reduced $[4Fe–4S]^{1+}$ cluster exists as a mixture of $S = \frac{1}{2}$ (20%) and $S = \frac{3}{2}$ (80%) ground states. From the presence of a strongly coupled ^1H ENDOR resonance in each case, it has been proposed that the noncysteine ligand is H_2O or OH^-, although the absence of a variation in $E^{0'}$ over the pH range 6.8–10.5 argues in favor of OH^- (*93*).

C. Investigating Cluster Reactivities in Adsorbed Protein Films

In the experiments described in Section III,B, application of two electrochemical methods, cyclic voltammetry and bulk electrolytic titration, facilitated the task of characterizing an unstable protein containing a labile Fe–S cluster. Even so, a considerable improvement in the exploratory and analytical capabilities of voltammetry may be achieved by addressing protein molecules that are confined to the electrode surface. Certain advantages of this approach have been outlined in the previous section.

The voltammograms in Fig. 11 show how an electroactive film of *D. africanus* Fd III (in this case the 7Fe form, as isolated) can be formed and stabilized at a PGE electrode in the presence of neomycin. In the first case, a freshly polished electrode is smeared with an ice-cold solution of protein (100 μM) from a capilliary tube, then transferred to electrolyte in an electrochemical cell and voltammetrically scanned. Only an initial weak response is observed. If neomycin (2 mM) is included in the coating solution (but still absent from the cell electrolyte), a voltammetric response is observed that dies away rapidly upon repeated cycling. However, if neomycin is present also in the cell electrolyte, the response is considerably stabilized after several cycles, thereafter undergoing only slow attenuation with time. The observa-

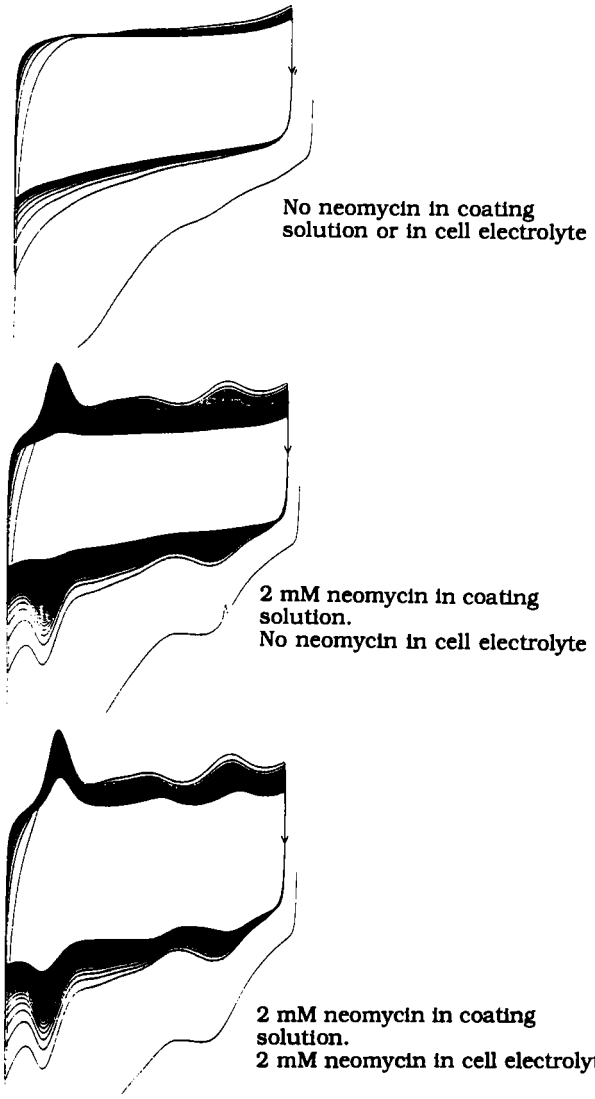

FIG. 11. Top: cyclic voltammograms (successive cycles) of a freshly polished PGE electrode coated with a drop (~1 μl) of a solution of *D. africanus* Fd III (100 μM in 0.1 *M* NaCl, 20 m*M* mixed buffer, 0.1 m*M* EGTA, pH 7) and scanned in the same electrolyte solution. Scan rate 190 mV/sec. Center: as for top voltammogram but 2 m*M* neomycin present in coating solution. Bottom: as for center but 2 m*M* neomycin present in cell solution.

tion is consistent with the formation of a protein layer in which the molecules are stabilized by the coadsorption of neomycin. Other ferredoxins, including *A. chroococcum/A. vinelandii* Fd I, exhibit similar behavior, and other aminocyclitols have been found to be active to varying extents (*87*). The structure of such films is clearly a complicated issue, but we have been able to exploit the situation to define several interesting reactions of [3Fe–4S] clusters and their derivatives.

After several cycles, the voltammetry of a film of 7Fe *D. africanus* Fd III appears as shown in Fig. 12. Based upon the close correspondence with the voltammetric waves A and B observed for solutions of the protein, the wave pairs A′ and B′ were assigned to the couples $[3Fe–4S]^{1+/0}$ and $[4Fe–4S]^{2+/1+}$, respectively (*35, 77*). It may be noted that ΔE_p values are small, (e.g., <30 mV at 190 mV/sec), thus indicating that electron transfer between the electrode and clusters approaches reversibility. Half-height widths (typically 100 and 120 mV, respectively) are close to theoretically expected values for a homogeneous population of noninteracting one-electron systems (see discussion in Section II,C). Furthermore, integration of these waves yields a value for the transferred charge that is consistent with the formation of approximately a one-protein monolayer. The third and most prominent wave pair C′ coincides with the appearance of C, a minor feature in the solution electrochemistry. This suggested that the redox process responsible for C′ occurs readily only in adsorbed protein molecules.

From a number of studies with other ferredoxins, it has become apparent that the low-potential couple C′ is associated closely with the presence of a [3Fe–4S] cluster. For example, a similar feature is evident for *A. chroococcum/A. vinelandii* Fd I and for the 7Fe proteins from *Sulfolobus acidocaldarius* and *Thermoplasma acidophilum* (*73, 76, 87*). For *D. africanus* Fd III, this proposal was supported further by the observation that both couples A and C vanish if the $[3Fe–4S]^0$ cluster is transformed by uptake of Fe(II), and by the absence of cysteine residues, additional to those required for cluster binding, that might constitute a redox-active cysteine/cystine redox couple. The positions and shapes of the reduction and oxidation waves were found to be dependent upon scan rate and upon pH (*77*). As the pH is lowered (e.g., below pH 7) and at slower scan rates, it was observed that ΔE_p decreases and the two waves become similar in shape with half-height widths less than 60 mV. The two-electron nature of this reaction has been confirmed by a series of comparisons of the integrated areas of oxidation waves A′ and C′ (*77*). Within experimental error, the charge passed for C′ is twice that for couple A′.

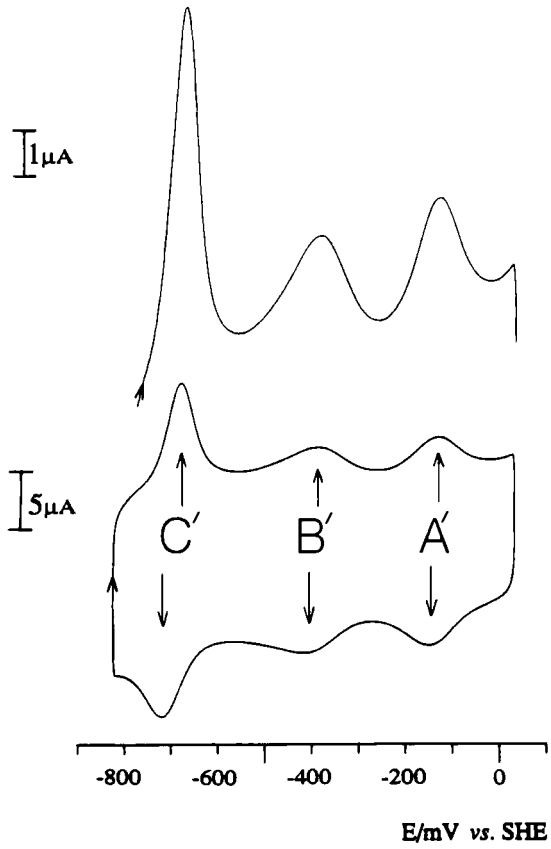

FIG. 12. Steady-state cyclic voltammogram of a film of *D. africanus* Fd III scanned in 0.1 *M* NaCl, 20 m*M* mixed buffer, pH 7, containing 2 m*M* neomycin and 10 m*M* EGTA. Temperature 0°C; scan rate 190 mV/sec. Upper trace is an oxidative scan measured at higher gain. [Reproduced from Butt, J. N., Armstrong, F. A., Breton, J., George, S. J., Thomson, A. J., and Hatchikian, E. C., *J. Am. Chem. Soc.* **113**, 6663 (1991), with permission.]

The nature of the reduced product of C′ remains unclear up to the time of preparing this manuscript. It is reasonably stable, as evident from the appearance of the oxidation wave even after holding the potential of the film-coated electrode below −850 mV for several minutes. Furthermore, it does not undergo turnover with evolution of H_2 (which should be thermodynamically favored under these conditions of very low potential). The most likely (yet still remarkable) rationale is that

the species $[3Fe–4S]^0$ itself is reducible by a further two electrons, as described by Eq. (7). This would give a cluster that is composed formally of three Fe(II).

$$[3Fe–4S]^0 + 2e^- - xH^+ \rightleftharpoons [3Fe–4S]^{2-}\text{---}xH^{8} \quad (7)$$

In recent studies, the reduction potential for Reaction (7) (as gauged from the average position of anodic and cathodic peaks) has been found to vary with pH (range 4.5–8.3) in an almost linear manner with a gradient corresponding to $x = 3$, i.e., suggesting that couple C′ as observed for *D. africanus* Fd III is a $2e^-/3H^+$ process (*87*).

As outlined earlier, it is widely recognized that the redox chemistry of [2Fe–2S] and [4Fe–4S] clusters in proteins is controlled tightly by the environment and is restricted to one-electron transitions between two adjacent oxidation levels (*84*). It now appears possible that [3Fe–4S] clusters are not so restricted. An important factor must be the accompanying binding of H^+ (possibly to bridging sulfides?) that compensates for the change in charge. However, the reason(s) why this reactivity appears confined to adsorbed protein molecules (at least in the case of *D. africanus* Fd III and *A. chroococcum/A. vinelandii* is not clear. Adsorption may assist complicated electrode reactions that involve successive electron transfers separated by a chemical rearrangement. Another possibility is that a rapid and reversible alteration of the cluster environment is induced under the condition of very low applied potential.

The adsorbed-film approach has provided a good way to explore the reactivity of the [3Fe–4S] cluster of *D. africanus* Fd III toward uptake of Fe(II) and other metals ions, under finely controlled conditions of applied potential (*35, 36, 87*). In a typical experiment, following film preparation and precycling in an EGTA-containing electrolyte solution, the electrode is transferred to another cell containing a known concentration of the metal ion to be tested. Reactivity may be controlled by varying the potential range or by applying routines in which the potential is held at certain values for periods of time. Cluster transformations are monitored and analyzed through changes in the appearance of the voltammogram. Following transfers of an electrode coated with a film of 7Fe *D. africanus* Fd III to solutions of Fe(II), Zn(II), and Cd(II), dramatic changes are observed over several rapid cycles (*35*). Some results are shown in Fig. 13, in which only the oxidative sweeps are displayed.

Couples A′ and C′ disappear to be replaced in each case by a single new couple D′, the reduction potential of which depends markedly upon the identity of the metal ion. Correspondence between the disappear-

ance of waves A′ and C′ and the appearance of waves D′ was established by comparing differential current amplitudes (expressed logarithmically) as an arbitrary function of time (cycle number). The reactions were found to proceed in a first-order manner, to an equilibrium position that is dependent upon the concentration of the particular metal ion. Estimated integrated areas of waves D′ and widths at half-height were similar to values observed for the original waves A′. Waves B′ were found to be unaffected. The semilog plots and resulting final voltammograms obtained under conditions of high metal ion concentration are also shown in Fig. 13. Interestingly, it was observed that the reactions with Cd and Zn were complete at much lower metal ion concentrations than was the case with Fe. This will be discussed further below.

As with the incorporation of Fe(II) described earlier, it was confirmed that reactions of *D. africanus* Fd III with Zn(II) or Cd(II) occurred with "free," i.e., unadsorbed, protein molecules (*35*). Bulk electrolytic titrations analogous to the type carried out to quantify Fe(II) incorporation showed that one equivalent of Zn(II) or Cd(II) was taken up by the $[3Fe–4S]^0$ form of the protein. Comparisons of $E^{0'}$ measured for films and for stoichiometrically transformed solutions are given in Table II. The close correspondence between reduction potentials determined for solution and film indicates that *D. africanus* Fd III molecules adsorbed at the electrode surface, under conditions of applied potential down to at least −600 mV, maintain cluster environments that are little perturbed from the native state. On the basis of EPR and MCD spectroscopic examination, it was proposed that the reaction products are $[Zn3Fe–4S]^{2+/1+}$ and $[Cd3Fe–4S]^{2+/1+}$ clusters. Two-electron reduced protein samples electrolysed at potentials of −535 and −650 mV, respectively, gave EPR spectra with signals around $g = 2$ (double integration giving ≤1 spin per molecule) and at $g = 4–5$. The former signals were assigned to the indigenous $[4Fe–4S]^{1+}$ cluster, i.e., couple B (B′), whereas the latter signals were assigned to the transformed product $[M3Fe–4S]^{1+}$, specifically the $M_s = \pm\frac{3}{2}$ middle Kramers' doublet of an $S = \frac{5}{2}$ state. In support of this, two weaker signals could be observed at low field ($g = 9.6$ and ~8.8) as predicted for the $M_s = \pm\frac{5}{2}$ and $\pm\frac{1}{2}$ doublets. The new spectral features resembled those assigned to the $[Zn3Fe–4S]^{1+}$ cluster that can be formed in *D. gigas* ferredoxin II (*33*). As shown by MCD spectroscopy, the oxidized species $[Zn3Fe–4S]^{2+}$ and $[Cd3Fe–4S]^{2+}$ each have the ground state $S = 2$. Spectra of each species are similar in the visible region (which is dominated by transitions due to the $[3Fe–4S]^0$ core) but differ in the region below 400 nm, where localized transitions, for example, $d^{10} \rightarrow s(p)$ or $S^{2-} \rightarrow$ Cd(II), are expected.

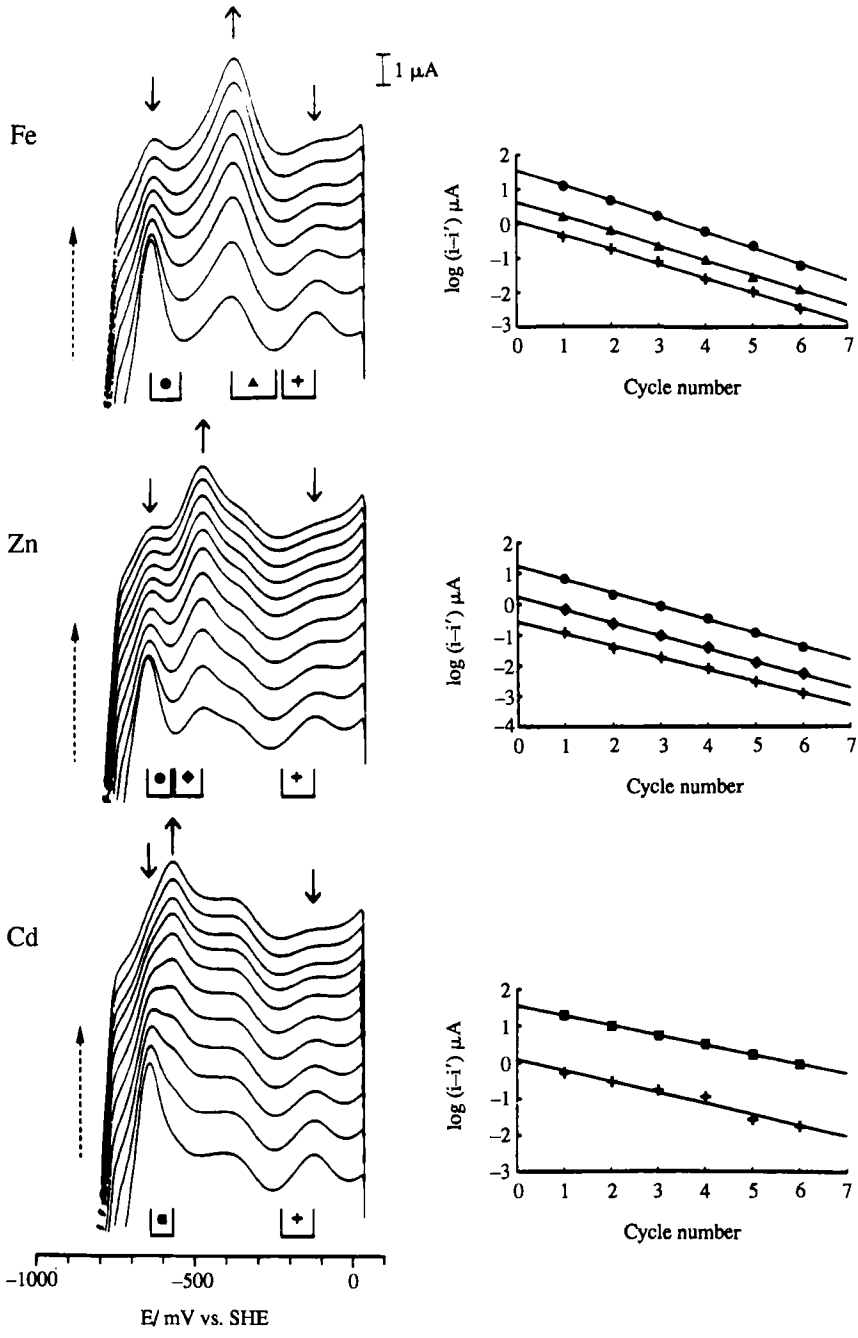
Fe
Zn
Cd
1 μA
log (i–i') μA
Cycle number
E/ mV vs. SHE
–1000
–500
0

TABLE II

$E^{0'}$ VALUES FOR FILMS AND TRANSFORMED SOLUTIONS[a]

		$E^{0'}$ (mV vs. SHE)	
[M3Fe–4S]	K_d (μM)	Film	Bulk
$[4Fe–4S]^{2+}$	30 ± 15	−393	−400
$[Zn3Fe–4S]^{2+}$	1.6 ± 1.0	−492	−480
$[Cd3Fe–4S]^{2+}$	0.8 ± 0.5	−569	−580
$[Tl3Fe–4S]^{1+}$	1.5 ± 1.0	—	—
$[Tl3Fe–4S]^{2+}$	34 mM	+81	—

[a] Upper set: values of voltammetrically determined dissociation constants K_d for Eq. (8) and comparison of reduction potentials $E^{0'}$ for the corresponding couple D′ ($[M3Fe–4S]^{2+/1+}$) as measured from film and bulk solution voltammetry of *D. africanus* Fd III. Conditions: 0.1 M NaCl, 20 mM mixed buffer as electrolyte; pH 7–7.4; temperature 0°C (film), 3–4°C (bulk). Data taken from Ref. *35*. Lower set: values of dissociation constants K_d for equilibrium of Tl(I) with the [3Fe–4S] cluster in a film of *D. africanus* Fd III. Conditions: 0.5 M Na/Tl acetate as electrolyte; pH 7; temperature 7°C. Data taken from Ref. *36*.

These reactions were shown to be reversible by transferring electrodes coated with transformed films back to electrolyte solutions containing no metal ion (*87*). As shown in Fig. 14, upon repeated cycling, the voltammogram of the original 7Fe ferredoxin reappears upon repeated cycling in the potential region favoring the presence of the

FIG. 13. Left: oxidative scans (successive cycles) of a film of 7Fe *D. africanus* Fd III upon transfer to M^{2+} solutions. Conditions otherwise as given for Fig. 12. Right: corresponding semilog plots showing time correspondence of appearance of waves D′ and disappearance of waves A′. The potential was held briefly at ~+50 mV prior to commencement of scanning at 470 mV/sec. Each determination involved measurement of the difference in current at two potentials as indicated. Fe^{2+} (300 μM): +, $i_{-129\,mV} - i_{-229\,mV}$, couple A′; ▲, $i_{-393\,mV} - i_{-250\,mV}$, couple D′; ●, $i_{-651\,mV} - i_{-554\,mV}$, couple C′. Zn^{2+} (10 μM): +, $i_{-129\,mV} - i_{-229\,mV}$, couple A′; ▲, $i_{-484\,mV} - i_{-570\,mV}$, couple D′; ●, $i_{-655\,mV} - i_{-579\,mV}$, couple C′. Cd^{2+} (10 μM): +, $i_{-129\,mV} - i_{-229\,mV}$, couple A′; ■, $i_{-641\,mV} - i_{-568\,mV}$, combination of couples C′ and D′. [Reproduced from Butt, J. N., Armstrong, F. A., Breton, J., George, S. J., Thomson, A. J., and Hatchikian, E. C., *J. Am. Chem. Soc.* **113**, 6663 (1991), with permission].

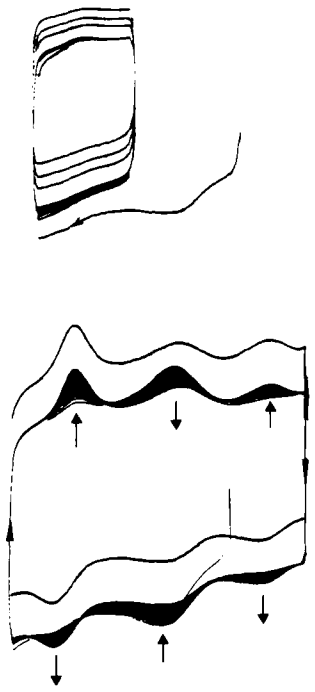

FIG. 14. Cyclic voltammograms showing release of Fe(II) from the transformed [4Fe–4S] cluster of *D. africanus* Fd III. Conditions as given for Fig. 13 but electrolyte contains no divalent metal ion. Top: cycling at 470 mV/sec restricted to potential region below −500 mV. There is no reappearance of couple C′ over a period of 10 min. Bottom: cycling at 470 mV/sec now including potential region in which transformed [4Fe–4S] cluster is oxidized. Couples A′ and C′ reappear within a minute.

oxidized cluster $[M3Fe–4S]^{2+}$. Metal ion release is not observed if cycling is restricted to the potential region in which [M3Fe–4S] remains in the +1 oxidation level. This shows that the reduced tetrametal cluster is more stable than the oxidized cluster with respect to release of the exchangeable metal ion. One way of viewing this is in terms of the immediate product $[3Fe–4S]^{1-}$ for which there is no evidence for stability. The observation emphasizes the importance of the environmental electrochemical potential in controlling such cluster transformations as they may occur *in vivo*.

At this juncture, it is appropriate to summarize the chemistry established to date for the two Fe–S clusters of *D. africanus* Fd III. The reactions are outlined in Fig. 15. The [3Fe–4S] cluster exhibits a wide and interesting reactivity, showing unusual capabilities for extensive electron/proton transfer and, in addition, undergoing facile, reversible

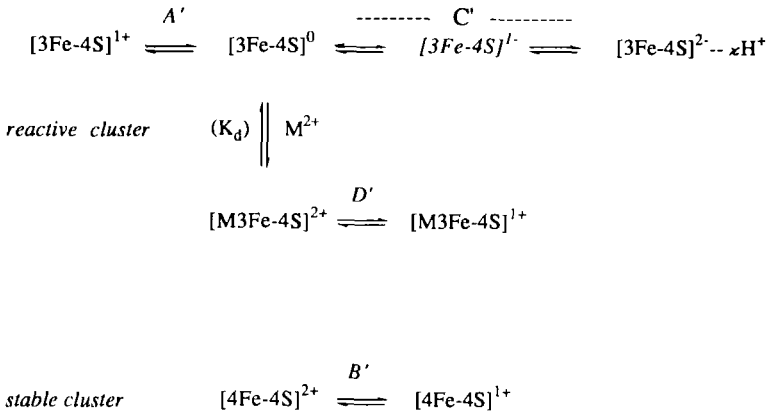

FIG. 15. Scheme showing the identities of couples A', B', C', and D' as observed in voltammetry of films of *D. africanus* Fd III.

incorporation of certain divalent and monovalent (see below) metal ions.

Reversible binding of divalent metal ions M^{2+} to the [3Fe–4S]^0 cluster is described by Eq. (8),

$$[M3Fe\text{–}4S]^{2+} \rightleftharpoons [3Fe\text{–}4S]^0 + M^{2+} \qquad K_d \tag{8}$$

for which the dissociation constant K_d is given by

$$K_d = \{[3Fe\text{–}4S]^0\}\{M^{2+}\}/\{[M3Fe\text{–}4S]^{2+}\} \tag{9}$$

and

$$\{[M3Fe\text{–}4S]^{2+}\}/\{[3Fe\text{–}4S]^0\} = \{M^{2+}\}/K_d \tag{10}$$

in which $\{M3Fe\text{–}4S]^{2+}\}$ and $\{[3Fe\text{–}4S]^0\}$ are surface populations (typically picomole or lower) and $\{M^{2+}\}$ is the solution concentration of metal ion. Equilibrium (dissociation) constants for these reactions were determined by measuring voltammetric signal amplitudes observed in a rapid cycle following equilibration of the film at a fixed potential in electrolyte solutions containing various concentrations of M^{2+}. Such a method is applicable if the rates of entry and release of Fe(II), Zn(II), and Cd(II) are slow compared to the voltammetric scan rates used. By carrying out such a determination under conditions of controlled potential, it could be ensured that the oxidation levels of each cluster species are as required by Eq. (9). From Eq. (10), a plot of the observed ratio $\{[M3Fe\text{–}4S]\}/\{[3Fe\text{–}4S]\}$ (oxidation levels omitted) against $\{M^{2+}\}$ is expected to yield a straight line with slope $1/K$.

Some results are illustrated in Fig. 16. A clearer distinction between the similar affinities displayed for Zn and Cd was made by direct competition experiments in which a film was transferred to solutions containing 1 : 1 and 2 : 1 (micromolar) ratios of the two ions. In the former case, the voltammogram was dominated by the appearance of the couple $[Cd3Fe–4S]^{2+/1+}$; in the latter case the couple $[Zn3Fe–4S]^{2+/1+}$ appeared at equal magnitude. The $[3Fe–4S]^0$ cluster in *D. africanus* Fd III thus displays the affinity order Cd ≥ Zn ≫ Fe. This comes as no surprise, since it is indeed the result that we expect from consideration of the Irving–Williams order (*94*). While it must be stressed that the nature of the noncluster ligand is not established [water (H_2O/OH^-) and aspartate are most likely], the identification of one example in which a $[3Fe–4S]^0$ cluster favors Zn(II) over Fe(II) by more than one order of magnitude implies an interesting and important viability of [Zn3Fe–4S] clusters in biological systems, for which Zn levels may approach (or even exceed) levels of Fe (*95, 96*). This possibility certainly requires further investigation, particularly since the EPR spectra reported for $[Zn3Fe–4S]^{1+}$ clusters differ so much from those normally observed for $[4Fe–4S]^{1+}$. Such heterometal species might readily escape

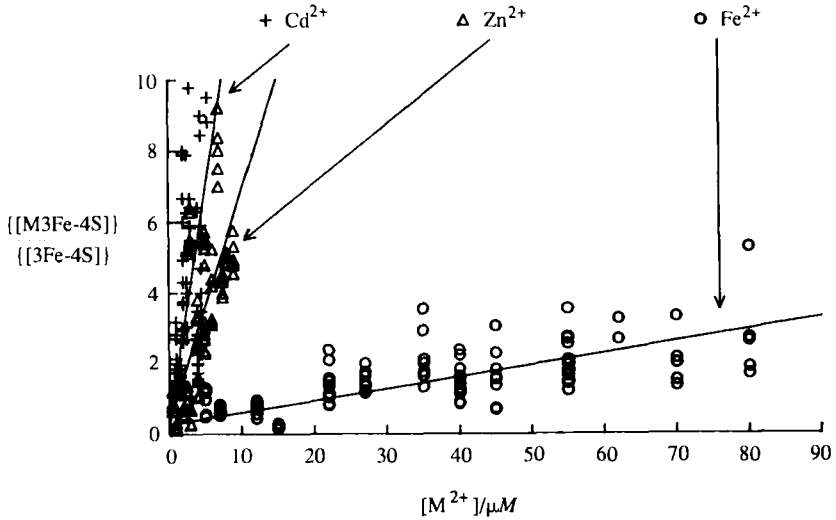

FIG. 16. Graph showing the dependence of the cluster population ratio {[M3Fe–4S]}/{[3Fe–4S]} for a film of *D. africanus* Fd III upon the concentration of metal ions in the electrolyte $\{M^{2+}\}$. [Adapted from Butt, J. N., Armstrong, F. A., Breton, J., George, S. J., Thomson, A. J., and Hatchikian, E. C., *J. Am. Chem. Soc.* **113**, 6663 (1991), with permission.]

attention. Without further structural information to reveal the nature of the noncluster ligation in each case, it is difficult to rationalize the large variation in reduction potentials that is observed. Such a variation, however, requires that the environmental electrochemical potential should be an important factor for controlling speciation in the presence of different metal ions.

An interesting extension of this theme is provided by the reaction of the [3Fe–4S] cluster of *D. africanus* Fd III with Tl(I) ions (*36*). This is an interesting example in which metal ion uptake and release is very fast, and occurs measurably for $[3Fe–4S]^{1+}$ in addition to $[3Fe–4S]^{0}$. Figure 17 shows how the position of couple A′ varies with the concentration of Tl(I) in the cell electrolyte. Waves B′ are unaffected, although Tl(0) deposition interferes with observation of waves C′. No such shifts were observed if 0.1 *M* K^+ (radius 138 pm) or 0.1 *M* Rb^+ (radius 152 pm) was substituted for Tl^+ (radius 150 pm). Competition experiments showed further that Tl(I) inhibits the coordination of Fe(II) at $[3Fe–4S]^{0}$.

Since the tri-μ-sulfido cluster face provides the only polarizable ligand group on the protein likely to be so selective for Tl^+ over similarly sized alkali metal ions, it was proposed that Tl(I) coordinates to the [3Fe–4S] core. The sigmoidal dependence of $E^{0'}$ upon Tl(I) concentra-

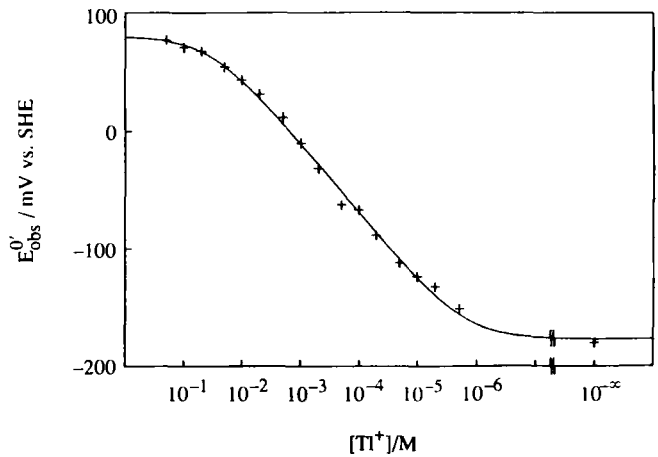

FIG. 17. Graph of observed reduction potentials for couple A′ (*D. africanus* Fd III) as a function of the concentration of Tl(I) in the electrolyte. The curve is the computed nonlinear regression fit to Eq. (11). [Reproduced from Butt, J. N., Sucheta, A., Armstrong, F. A., Breton, J., Thomson, A. J., and Hatchikian, E. C., *J. Am. Chem. Soc.* **113**, 8948 (1991), with permission.]

tion was rationalized in terms of the cyclic reaction scheme shown in Fig. 18, in which electron transfer is coupled to very rapid uptake and release of Tl(I). This type of situation, in which species equilibrate rapidly within the voltammetric scan time, is analogous to a potentiometric experiment. Values of K_d^{ox}, K_d^{red}, and $E_{Tl}^{0'}$ are obtained from application of Eqs. (11) and (12). Results are included in Table II.

$$E_{obs}^{0'} = E^{0'} + (2.303\,RT/F)\log\{(1 + [Tl^+]/K_d^{red})/(1 + [Tl^+]/K_d^{ox})\} \quad (11)$$

$$E_{Tl}^{0'} = E^{0'} + (2.303\,RT/F)\log(K_d^{ox}/K_d^{red}) \quad (12)$$

The proposal that Tl(I) enters the [3Fe–4S] core was supported by spectroscopic studies (*36*). With a $[Tl^+]$ concentration of 133 m*M* (i.e., a fourfold excess over the determined value of K_d^{ox}), the characteristic $g = 2.01$ signal of $[3Fe–4S]^{1+}$ was replaced by a rhombic spectrum having g values 2.04, 1.99, and 1.95. Intermediate concentrations of Tl(I) produced spectra that were superpositions of the new species and of $[3Fe–4S]^{1+}$. The K_d^{ox} value estimated from these spectra was in good agreement with that determined from the film voltammetry. As with other transformation products, the identity of the noncluster ligand(s) to the Tl site has not been established at the time of preparing this manuscript.

The results highlight several new features. First, they demonstrate the existence of a possible biological target for Tl(I), a known toxic element (*97*); indeed the affinity of Tl(I) for $[3Fe–4S]^0$ is much stronger than reported affinities for Tl(I) occupancy of K^+ sites (*98*). Second, they demonstrate the interaction of a monovalent ion with a [3Fe–4S] cluster. Third, by conforming well to a rapid equilibrium model, even

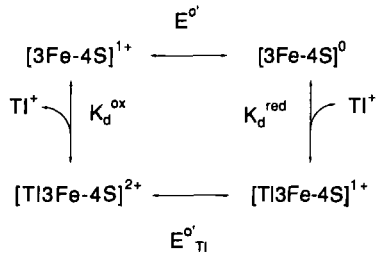

FIG. 18. Scheme showing reversible binding of Tl(I) to +1 and 0 oxidation levels of the [3Fe–4S] cluster of *D. africanus* Fd III. [Reproduced from Butt, J. N., Sucheta, A., Armstrong, F. A., Breton, J., Thomson, A. J., and Hatchikian, E. C., *J. Am. Chem. Soc.* **113,** 8948 (1991), with permission.]

at a scan rate of 470 mV/sec, it can be concluded that both "on" and "off" rates for binding of Tl(I) are very fast. This implies that the metal-binding site at the [3Fe–4S] cluster of *D. africanus* Fd III is probably exposed to solvent and that the protein does not resist the transformation. The implication that this access is not restricted significantly (if at all) by the adsorbed state of the protein molecule indicates also that there is considerable fluidity within the protein/aminocyclitol film.

A brief, final illustration of the use of adsorbed film voltammetry is the ability to study rapid interactions of clusters with extraneous ligands (*99*). From these experiments, as before, new species can be detected and their limits for existence defined to allow isolation and structural characterization. Figure 19 shows the voltammetry that results following transfer of an PGE electrode coated with a Fe-transformed film of *D. africanus* Fd III into a solution containing 0.54 *M* mercaptoethanol. The observations may be rationalized in terms of the generic scheme shown in Fig. 20, in which rapid and reversible binding of a ligand L occurs to both the 2+ and 1+ oxidation levels of a [M3Fe–4S] cluster [M is a divalent metal, in this case Fe(II)].

Under conditions of rapid scan rate (1 V/sec) waves D′, which are normally coincident with waves B′ if M = Fe, are replaced by a couple (termed F′) for which the reduction potential $E_F^{0'} = -585$ mV. The shift in potential is thus approximately −190 mV. The amplitudes of reduction and oxidation waves F′ are similar at this scan rate, but do depend upon pH and mercaptoethanol concentration; under the conditions used for this particular experiment, their amplitude is comparable with waves B′. By contrast, under conditions of slow scan rate (10 mV/sec), D′ is replaced by a new couple having an apparent reduction potential $E_{obs}^{0'}$ that is dependent upon pH and mercaptoethanol concentration. The amplitudes of reduction and oxidation waves are equal, and independent of mercaptoethanol concentration. The two experiments relate to kinetically limiting cases for the scheme shown in Fig. 20. Examination of the effect of pH shows that the active ligand L is ethanol-2-thiolate (the pK of mercaptoethanol under these conditions is 9.8). In the fast scan experiment, ligand binding and release is effectively frozen and the voltammogram displays the isolated couples F′ and D′ (overlaid on B′; little or no D′ is actually observed under the conditions used). In the slow scan limit, equilibrium conditions are established for ligand interaction and the voltammetry becomes analogous to a potentiometric experiment. The observed reduction potential $E_{obs}^{0'}$ is related to ligand concentration ([thiolate] = ([total thiol])/(1 + $[H^+]/10^{-9.8}$)) by equations analogous to those given in Eqs. (11) and (12) for Tl^+ binding to $[3Fe–4S]^{1+/0}$. Data analysis shows that the

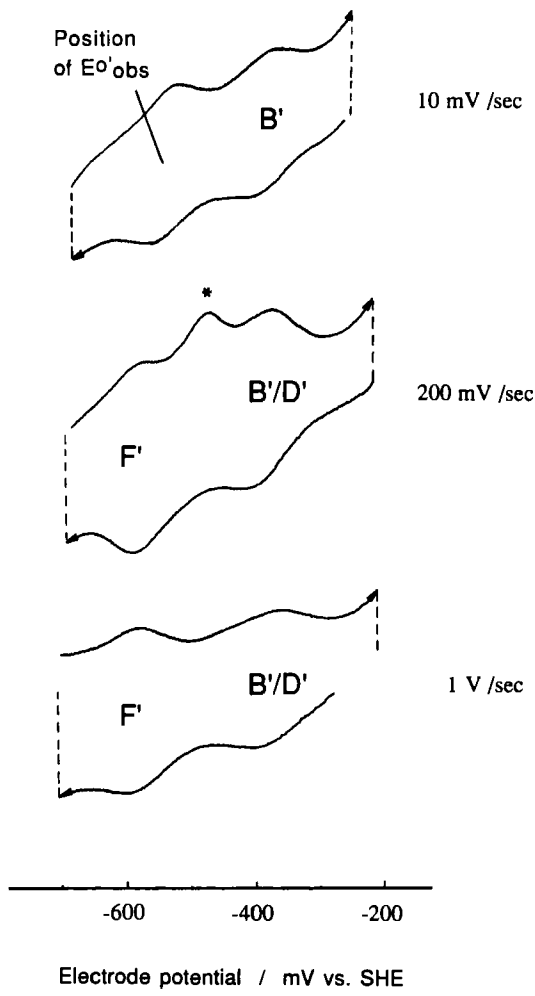

FIG. 19. Cyclic voltammograms at various scan rates, of a pretransformed film of 8Fe *D. africanus* Fd III contacting a solution of Fe(II) (180 μM) and mercaptoethanol (0.54 M). Conditions: electrolyte consists of 0.2 M NaCl, 20 mM Tris HCl, 2 mM neomycin, pH 8; temperature 0°C. In each case the charging current contribution has been trimmed to aid visual comparison. All scans commence from the high-potential limit.

reduced cluster $[4Fe–4S]^{1+}$ displays a much lower affinity for the ligand ($K^{red}_{d(L)}$ = 96 mM) than does the oxidized cluster ($K^{ox}_{d(L)}$ = 30 μM). At the time of writing, it is not established whether L replaces an incumbent ligand or adds to increase the coordination number of the target subsite. The M subsite is implicated since voltammetry of the

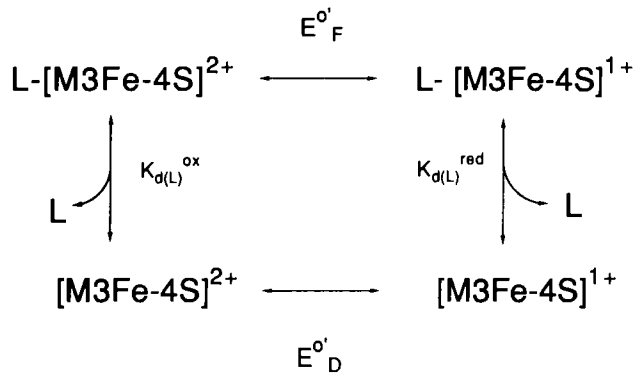

FIG. 20. Scheme showing reversible binding of an extraneous ligand L to 2+ and 1+ oxidation levels of a [M3Fe–4S] cluster (M is a divalent metal ion). All parameters may be determined from the voltammetry.

untransformed 7Fe protein measured in mercaptoethanol is unperturbed. The observations for *D. africanus* Fd III thus provide a further demonstration that incorporation of M into a [3Fe–4S] cluster itself generates new chemical reactivity that may be important in the stabilization of proteins and protein adducts.

Voltammograms measured at intermediate scan rates reveal the kinetics of ligand interaction. Substantial release of L from $[4Fe–4S]^{1+}$ is evident from inspection of Fig. 19 (center) which shows a much attenuated reoxidation wave for F'. A third oxidation wave (*) is now observed which corresponds to the coupled rapid recombination of the electrode product $[4Fe–4S]^{2+}$ with L. It is noted that the *total* amount of charge passed between the electrode and protein during each scan remains constant. Such voltammograms clearly contain a wealth of information that should be readily extractable using computer simulation methods.

IV. Conclusions

In what is a limited number of experiments described in this Section, I hope to have shown or at least hinted at several useful and interesting aspects of direct electrochemical methods as applied to the problems of Fe–S clusters. The examples given should serve as some demonstration that the techniques can be effective and may have wide application in the area.

It has proved straightforward to detect redox couples at potentials far below the limits of dithionite at neutral pH, to study the stabilities of the reduced species, and to generate samples in specific states of reduction for spectroscopy. Voltammetric signals have been used as signatures of cluster status, appropriate for time domain investigations.

The adsorbed film studies described for *D. africanus* Fd III illustrate a new strategy for studying proteins with very reactive Fe–S clusters. The approach combines high sensitivity, accuracy, and the ability to study reactions under strict conditions of applied potential. Complex, seemingly erratic behavior can be managed and visualized. Equilibrium and kinetic data may be derived with just trace amounts of protein, and verified by preparation of appropriate spectroscopic samples. From the results of spectroscopic studies on the products of parallel transformations carried out in solution, it is indeed demonstrated that the voltammetric interrogation of Fe–S proteins in an adsorbed film can provide an acceptably valid reflection of the chemistry of free molecules. A useful "trailblazing" capability is thus provided to give guidance and to complement the techniques aimed at detailed structural characterization.

ACKNOWLEDGMENTS

The author thanks a number of co-workers who have been closely involved with most of the studies described in this article. These include J. N. Butt, S. J. George, J. Breton, A. Vásquez, A. Sucheta, A. J. Thomson, E. C. Hatchikian, R. Cammack, B. K. Burgess, and P. J. Stephens. Funding from the SERC (UK), The Royal Society, from the Exxon Education Foundation, and the ACS Petroleum Research Fund is gratefully acknowledged.

REFERENCES

1. Armstrong, F. A., Hill, H. A. O., and Walton, N. J., *Acc. Chem. Res.* **21,** 407 (1988).
2. Armstrong, F. A., *Struct. Bonding* **72,** 137 (1990).
3. Guo, L. H., and Hill, H. A. O., *in* "Advances in Inorganic Chemistry" (A. G. Sykes, ed.), Vol. 36, p. 341. Academic Press, San Diego, California, 1991.
4. Pielak, G. J., Concar, D. W., Moore, G. R., and Williams, R. J. P., *Protein Eng.* **1,** 83 (1987).
5. McLendon, G., *Acc. Chem. Res.* **21,** 160 (1988).
6. Williams, R. J. P., *Biochem. Int.* **18,** 475 (1989).
7. Lyklema, J., *Colloids Surf.* **10,** 33 (1984).

8. Dutton, P. L., *in* "Methods in Enzymology" (S. Fleischer and L. Packer, eds.), Vol. 54, p. 411. Academic Press, New York, 1978.
9. Bond, A. M., "Modern Polarographic Methods in Analytical Chemistry." Dekker, New York and Basel, 1980.
10. Bard, A. J., and Faulkner, L. R., "Electrochemical Methods, Fundamentals and Applications." Wiley, New York, 1980.
11. Kissinger, P. T., and Heineman, W. R., eds., "Laboratory Techniques in Electroanalytical Chemistry." Dekker, New York and Basel, 1984.
12. Southampton Electrochemistry Group, "Instrumental Methods in Electrochemistry." Ellis Horwood, Chichester, 1985.
13. Beinert, H., *FASEB J.* **4,** 2483 (1990).
14. Beinert, H., and Kennedy, M. C., *Eur. J. Biochem.* **186,** 5 (1989).
15. Rouault, T. A., Stout, C. D., Kaptain, S., Harford, J. B., and Klausner, R. D., *Cell (Cambridge, Mass.)* **64,** 881 (1991).
16. Hentze, M. W., and Argos, P., *Nucl. Acid Res.* **19,** 1739 (1991).
17. Beinert, H., and Thomson, A. J., *Arch. Biochem. Biophys.* **222,** 333 (1983).
18. Beinert, H., Emptage, M. H., Dreyer, J.-L., Scott, R. A., Hahn, J. E., Hodgson, K. O., and Thomson, A. J., *Proc. Natl. Acad. Sci. U.S.A.* **80,** 393 (1983).
19. Stephens, P. J., Morgan, T. V., Devlin, F., Penner-Hahn, J., Hodgson, K. O., Scott, R. A., Stout, C. D., and Burgess, B. K., *Proc. Natl. Acad. Sci. U.S.A.* **83,** 5661 (1985).
20. Antonio, M. R., Averill, B. A., Moura, I., Moura, J. J. G., Orme-Johnson, W. H., Teo, B.-K., and Xavier, A. V., *J. Biol. Chem.* **257,** 6646 (1982).
21. Stout, C. D., *J. Mol. Biol.* **205,** 545 (1989).
22. Stout, G. H., Turley, S., Sieker, L. C., and Jensen, L. H., *Proc. Natl. Acad. Sci. U.S.A.* **85,** 1020 (1988).
23. Kissinger, C. R., Sieker, L. C., Adman, E. T., and Jensen, L. H., *J. Mol. Biol.* **219,** 693 (1991).
24. Stephens, P. J., Jensen, G. M., Devlin, F. J., Morgan, T. V., Stout, C. D., Martin, A. E., and Burgess, B. K., *Biochemistry* **30,** 3200 (1991).
25. Gurbiel, R. J., Batie, C. J., Sivaraja, M., True, A. E., Fee, J. A., Hoffman, B. M., and Ballou, D. P., *Biochemistry* **28,** 4861 (1989).
26. Robbins, A. H., and Stout, C. D., *Proc. Natl. Acad. Sci. U.S.A.* **86,** 3639 (1989).
27. Werst, M. M., Kennedy, M. C., Beinert, H., and Hoffman, B. M., *Biochemistry* **29,** 10526 (1990).
28. Moura, J. J. G., Moura, I., Kent, T. A., Lipscomb, J. D., Huynh, B.-H., LeGall, J., Xavier, A. V., and Münck, E., *J. Biol. Chem.* **257,** 6259 (1982).
29. George, S. J., Armstrong, F. A., Hatchikian, E. C., and Thomson, A. J., *Biochem. J.* **264,** 275 (1989).
30. Conover, R. C., Kowal, A. T., Fu, W., Park, J.-B., Aono, S., Adams, M. W. W., and Johnson, M. K., *J. Biol. Chem.* **265,** 8533 (1990).
31. Hagen, W. R., Pierik, A. J., and Veeger, C., *J. Chem. Soc., Faraday Trans. 1,* **85,** 4083 (1989).
32. Moura, I., Moura, J. J. G., Münck, E., Papaefthymiou, V., and LeGall, J., *J. Am. Chem. Soc.* **108,** 349 (1986).
33. Sureus, K. K., Münck, E., Moura, I., Moura, J. J. G., and LeGall, J., *J. Am. Chem. Soc.* **109,** 3805 (1987).
34. Conover, R. C., Park, J.-B., Adams, M. W. W., and Johnson, M. K., *J. Am. Chem. Soc.* **112,** 4562 (1990).
35. Butt, J. N., Armstrong, F. A., Breton, J., George, S. J., Thomson, A. J., and Hatchikian, E. C., *J. Am. Chem. Soc.* **113,** 6663 (1991).

36. Butt, J. N., Sucheta, A., Armstrong, F. A., Breton, J., Thomson, A. J., and Hatchikian, E. C., *J. Am. Chem. Soc.* **113,** 8948 (1991).
37. Burgess, B. K., *Chem. Rev.* **90,** 1377 (1990).
38. Eady, R. R., *in* "Advances in Inorganic Chemistry" (A. G. Sykes, ed.), Vol. 36, p. 77. Academic Press, San Diego, California, 1991.
39. Stack, T. D. P., and Holm, R. H., *J. Am. Chem. Soc.* **110,** 2484 (1988).
40. Ciurli, S., Carrié, M., Weigel, J. A., Carney, M. J., Stack, T. D. P., Papaefthymiou, G. C., and Holm, R. H., *J. Am. Chem. Soc.* **112,** 2654 (1990).
41. Holm, R. H., Ciurli, S., and Weigel, J. A., *Prog. Inorg. Chem.* **38,** 1 (1990).
42. Weigel, J. A., and Holm, R. H., *J. Am. Chem. Soc.* **113,** 4184 (1991).
43. Kovacs, J. A., and Holm, R. H., *Inorg. Chem.* **26,** 702, 711 (1987).
44. Ciurli, S., Carney, M. J., Holm, R. H., and Papaefthymiou, G. C., *Inorg. Chem.* **28,** 2696 (1989).
45. Ciurli, S., Carrie, M., and Holm, R. H., *Inorg. Chem.* **29,** 3493 (1990).
46. Ciurli, S., Yu, S.-B., Holm, R. H., Srivastava, K. K. P., and Münck, E., *J. Am. Chem. Soc.* **112,** 8169 (1990).
47. Mayhew, S. G., *Eur. J. Biochem.* **85,** 535 (1978).
48. Armstrong, F. A., Bond, A. M., Hill, H. A. O., Psalti, I. S. M., and Zoski, C. G., *J. Phys. Chem.* **93,** 6485 (1989).
49. Armstrong, F. A., Bond, A. M., Hill, H. A. O., Oliver, B. N., and Psalti, I. S. M. J., *J. Am. Chem. Soc.* **111,** 9185 (1989).
50. Buchi, F., and Bond, A. M., *J. Electroanal. Chem.*, in press (1992).
51. Nicholson, R. S., and Shain, I., *Anal. Chem.* **36,** 706 (1964).
52. Laviron, E., *J. Electroanal. Chem.* **52,** 355 (1974).
53. Laviron, E., *J. Electroanal. Chem.* **52,** 395 (1974).
54. Laviron, E., *J. Electroanal. Chem.* **101,** 19 (1979).
55. Osteryoung, J. G., and Osteryoung, R. A., *Anal. Chem.* **57,** 101A (1985).
56. Smith, E. T., and Feinberg, B. A., *J. Biol. Chem.* **265,** 14371 (1990).
57. Smith, E. T., Bennett, D. W., and Feinberg, B. A., *Anal. Chim. Acta* **251,** 27 (1991).
58. Crawley, C. D., and Hawkridge, F. M., *J. Electroanal. Chem.* **159,** 313 (1983).
59. Albery, W. J., Eddowes, M. J., Hill, H. A. O., and Hillman, A. R., *J. Am. Chem. Soc.* **103,** 3904 (1981).
60. Weitzman, P. D. J., Kennedy, I. R., and Caldwell, R. A., *FEBS Lett.* **17,** 241 (1971).
61. Dalton, H., and Zubieta, J., *Biochim. Biophys. Acta* **322,** 133 (1973).
62. Zuznetsov, B. A., Mestechkina, N. M., and Shumakovich, G. P., *Bioelectrochem. Bioenerg.* **4,** 1 (1977).
63. Hill, C. L., Renaud, J., Holm, R. H., and Mortenson, L. E., *J. Am. Chem. Soc.* **99,** 2549 (1977).
64. Bianco, P., and Haladjian, J., *Biochem. Biophys. Res. Commun.* **78,** 323 (1977).
65. Ikeda, T., Toriyama, K., and Senda, M., *Bull. Chem. Soc. Jpn.* **52,** 1937 (1979).
66. Van Dijk, C., Van Leeuwen, J. W., Veeger, C., Schreurs, J. P. G. M., and Barendrecht, E., *Bioelectrochem. Bioenerg.* **9,** 743 (1982).
67. Cotton, F. A., and Wilkinson, G., "Advanced Inorganic Chemistry," Wiley (Interscience), 5th Ed., p. 613. New York, 1988.
68. Landrum, H. L., Salmon, R. T., and Hawkridge, F. M., *J. Am. Chem. Soc.* **99,** 3154 (1977).
69. Bianco, P., Haladjian, J., Tobiana, G., Forget, P., and Bruschi, M., *Bioelectrochem. Bioenerg.* **12,** 509 (1984).
70. Van Dijk, C., Van Eijs, T., Van Leeuwen, J. W., and Veeger, C., *FEBS Lett.* **166,** 76 (1984).

71. Armstrong, F. A., Hill, H. A. O., and Walton, N. J., *FEBS Lett.* **145,** 241 (1982).
72. Armstrong, F. A., Cox, P. A., Hill, H. A. O., Lowe, V. J., and Oliver, B. N., *J. Electroanal. Interfac. Electrochem.* **217,** 331 (1987).
73. Armstrong, F. A., George, S. J., Thomson, A. J., and Yates, M. G., *FEBS Lett.* **234,** 107 (1988).
74. Rinehart, K. L., and Suami, T., eds., "Aminocyclitol Antibiotics," ACS Symp. Ser. Vol. 125, American Chemical Society, Washington, D.C., 1980.
75. Armstrong, F. A., George, S. J., Cammack, R., Hatchikian, E. C., and Thomson, A. J., *Biochem. J.* **264,** 265 (1989).
76. Iismaa, S. E., Vázquez, A. E., Jensen, G. M., Stephens, P. J., Butt, J. N., Armstrong, F. A., and Burgess, B. K., *J. Biol. Chem.* **266,** 21563 (1991).
77. Armstrong, F. A., Butt, J. N., George, S. J., Hatchikian, E. C., and Thomson, A. J., *FEBS Lett.* **259,** 15 (1989).
78. George, S. J., Richards, A. J. M., Thomson, A. J., and Yates, M. G., *Biochem. J.* **224,** 247 (1984).
79. Johnson, M. K., Bennett, D. E., Fee, J. A., and Sweeney, W. V., *Biochim. Biophys. Acta* **911,** 81 (1987).
80. Johnson, M. K., Thomson, A. J., Richards, A. J. M., Peterson, J., Robinson, A. E., Ramsay, R. R., and Singer, T. P., *J. Biol. Chem.* **259,** 2274 (1984).
81. Thomson, A. J., Robinson, A. E., Johnson, M. K., Moura, J. J. G., Moura, I., Xavier, A. V., and LeGall, J., *Biochim. Biophys. Acta* **670,** 93 (1981).
82. Morgan, T. V., Stephens, P. J., Devlin, F., Stout, C. D., Melis, K. A., and Burgess, B. K., *Proc. Natl. Acad. Sci. U.S.A.* **81,** 1931 (1984).
83. Hagen, W. R., Dunham, W. R., Johnson, M. K., and Fee, J. A., *Biochim. Biophys. Acta* **828,** 369 (1985).
84. Backes, G., Mino, Y., Loehr, T. M., Meyer, T. E., Cusanovich, M. A., Sweeney, W. V., Adman, E. T., and Sanders-Loehr, J., *J. Am. Chem. Soc.* **113,** 2055 (1991).
85. Armstrong, F. A., Hill, H. A. O., and Walton, N. J., *FEBS Lett.* **150,** 214 (1982).
86. Cammack, R., *Biochem. Biophys. Res. Commun.* **54,** 548 (1973).
87. Butt, J. N., and Armstrong, F. A., unpublished results (1991).
88. Soman, J., Iismaa, S., and Stout, C. D., *J. Biol. Chem.* **266,** 21558 (1991).
89. Martin, A. E., Burgess, B. K., Stout, C. D., Cash, V. L., Dean, D. R., Jensen, G. M., and Stephens, P. J., *Proc. Natl. Acad. Sci. U.S.A.* **87,** 598 (1990).
90. Bovier-Lapierre, G., Bruschi, M., Bonicel, J., and Hatchikian, E. C., *Biochim. Biophys. Acta* **913,** 20 (1987).
91. Hatchikian, E. C., Cammack, R., Patel, D. S., Robinson, A. E., Richards, A. J. M., George, S. J., and Thomson, A. J., *Biochim. Biophys. Acta* **784,** 40 (1984).
92. Otaka, E., and Ooi, T., *J. Mol. Evol.* **26,** 257 (1987).
93. Park, J.-B., Fan, C., Hoffman, B. M., and Adams, M. W. W., *J. Biol. Chem.* **266,** 19351 (1991).
94. Phillips, C. S. G., and Williams, R. J. P., "Inorganic Chemistry," Vol. 1, p. 630. Oxford Univ. Press, London and New York, 1965.
95. Ochiai, E.-I., "General Principles of Biochemistry of the Elements," Chap. 12. Plenum, New York, 1987.
96. Mills, C. F., ed., "Zinc in Human Biology." Springer-Verlag, Berlin, 1989.
97. Douglas, K. T., Bunni, M. A., and Baindur, S. R., *Int. J. Biochem.* **22,** 429 (1990).
98. Markham, G. D., Hafner, E. W., Tabor, C. W., and Tabor, H., *J. Biol. Chem.* **255,** 9082 (1980).
99. Butt, J. N., and Armstrong, F. A., unpublished results (1992).